

**Analysis of Lithologic Properties and Permeability Values in
Closely Spaced Cores from the Tonganoxie Sandstone,
Wyandotte County, Kansas**

D. Scott Beaty and Alex Martinez

Kansas Geological Survey Open-File Report 98-53

Introduction

This report summarizes the results of a coring study that examined ten closely spaced, near subsurface cores (NE SW NW, Sec. 8, T11S, R23E) in Wyandotte County, Kansas (Figure 1). These cores were drilled through the Tonganoxie Sandstone Member of the Stranger Formation (Upper Pennsylvanian, Douglas Group) behind the fluvial outcrop study site of Beaty et al. (1997) (Figure 2). The outcrop at the study site provided an opportunity to examine contacts between sandstone sets, analyze changes in grain size and mica distribution, and make closely spaced measurements of permeability at an interwell-scale. However, examination of the two-dimensional exposure provided little information about these properties away from the outcrop face. Study of the closely spaced cores made it possible to analyze the three-dimensional distribution of *in situ* air permeability (K_a) and lithologic types, such as sandstone and conglomerate, at an interwell-scale.

The Tonganoxie Sandstone accumulated within an incised paleovalley that extended across much of eastern Kansas during the early Virgilian (Figure 1). The valley-fill succession consists of very fine- to fine-grained sandstone facies overlain by a regionally developed succession of interbedded, heterolithic sandstone, siltstone, and shale facies (Archer et al. 1994; Feldman et al. 1995; Beaty, *in prep.*). Feldman et al. (1995) interpreted the depositional environments of sandstone facies in the Tonganoxie valley-fill. They divided the Tonganoxie Sandstone into four stratigraphic types: a basal conglomerate and braided-fluvial sheet sandstone (type 1), arcuate to sinuous estuarine point bar and channel sandstone (type 2), elongate pods of valley-head delta sandstone (type 3), and thin, discontinuous shallow marine sheet sandstone (type 4). Archer et al. (1994) described the stratigraphic architecture of Douglas Group sandstones and placed the Tonganoxie interval into a sequence stratigraphic framework. The Tonganoxie Sandstone is an important groundwater aquifer (O'Conner 1960), and is an analog for sandstone hydrocarbon reservoirs with similar architectural and petrologic characteristics (Beaty, *in prep.*).

Outcrop Description

Archer et al. (1993) determined that the sandstone at the outcrop was deposited in a type 1 fluvial setting. Beaty et al. (1997) analyzed K_a values and petrologic attributes of the sandstone. They divided the sandstone vertically into two intervals with similar characteristics. They determined that the hydrodynamic properties of the intervals were distinctively different, warranting their division into an upper and a lower flow unit.

The lower flow unit consists of trough cross-bedded (*S_t*) sets (Figure 3) in channel (CH) architectural elements (c.f. Miall 1985). Cross-cutting *S_t* sets are the result of repeated scouring and filling during sandstone deposition. The *S_t* sets contain very fine- to fine-grained, micaceous quartz sandstone. Small-scale studies of the outcrop face reveal that mica was more concentrated at the base of the *S_t* sets in lamina near trough scours, than in upper portions of the sets (Beaty et al. 1997; Beaty, *in prep.*). Beaty et al. (1997) used ground-penetrating radar (GPR) data from a grid of vertical profiles to determine the width and orientation of *S_t* sets and CH elements. The *S_t* sets are 5 to 10 m (16.4 to 32.8 ft) across and generally decrease in width upward. The axes of trough and channel scours trend toward the southeast, suggesting that the local paleotransport direction was parallel to this direction (Beaty et al. 1997).

The upper flow unit consists of *S_t* sets and low angle cross-bedded (*S_l*) sets containing silty, very fine- to fine-grained, highly micaceous quartz sandstone. Upper flow unit *S_t* sets are not as wide as lower flow unit *S_t* sets and are typically less than 5 m (16.4 ft) across. In the upper flow unit, trough axes of *S_t* sets have orientations that range from southeast to southwest.

At an exposure across the highway from the sandstone outcrop of Beaty et al. (1997), a conglomerate interval is present at the base of the Tonganoxie Sandstone above the lower sequence boundary of the Tonganoxie sequence (Archer et al. 1994). The conglomerate interval, which overlies 0.08 to 0.15 m (0.25 to 0.50 ft) of Weston Shale, consists of a 1 to 1.3 m (3.3 to 4.3 ft) interbedded succession of conglomerate, conglomeratic sandstone, and minor sandstone. This interval is commonly cemented with calcite and iron oxide or hydroxide, and has an undulating upper surface. Of the

lithologic types present, conglomerate beds dominate the succession. Some of the conglomerate beds are laterally continuous and can be traced for distances greater than 20 m (66 ft) along the outcrop face. These beds consist of a bimodal assemblage of granule to pebble-sized shale, limestone, and limonitic shale clasts, and minor wood fragments within a matrix of very fine- to fine-grained quartz sand. In conglomerate beds, clasts consist mostly of angular limestone fragments and lesser amounts of angular shale fragments that are up to 7 cm long. Clast abundance in these beds ranges from 20% to 70%. Clast sizes vary from bed to bed, with granular clasts dominant in some beds and angular pebble-sized clasts dominant in others. In conglomeratic sandstone beds, clasts are mostly less than 1 cm long and consist of rounded shale fragments and lesser amounts of angular limestone fragments.

Methods

Ten 6.4 cm (2.5 inch) diameter cores were drilled in a 4500 m² area (48,200 ft²) in the field behind the outcrop site (Figure 4). Six of the cores were drilled 16 m apart along an 80-meter-long northeast-trending transect. The other four cores were drilled 28 m away from the 6-core transect; two to the northwest and two to the southeast of the transect (Figure 4). Core T132 P014 was drilled approximately 18 m from the outcrop face and northeast of outcrop permeability Station 250. An outcrop profile containing permeability Station 250 is shown in Figure 3.

In the drill holes, wireline logs were used to determine conductivity and gamma ray values. Wireline log gamma ray and conductivity values from each hole are plotted as graphs on the core descriptions shown in Appendix 1 and in Plate 1.

A Temco Model MP-400 Electronic Field Gas Permeameter (minipermeameter) was used to make measurements of K_a values along the length of the cores. These K_a measurements were made at intervals that ranged from 7.5 cm to 15 cm (3 to 6 inches). Data collection and analysis methods for minipermeameter measurements are described in Beaty (*in prep.*). Appendix 2 includes the values of K_a determined with the minipermeameter and includes data used to calculate the values. Graphs of

these K_a values are shown on the left side of core descriptions in Appendix 1 and on the right side of the respective core description in Plate 1.

Horizontal K_a , porosity, and grain density values were measured for 37 plug samples drilled at 30.5 cm intervals (+ or - 6 cm) from cores T104 P014 and T132 P014, and for 8 plug samples from cores T104 P062 and T104 P078. In the laboratory, a permeameter equipped with a Hassler-type sample chamber was used to measure K_a values for the cores, and a helium porosimeter was used to measure porosity and grain density. Porosity, grain density, and K_a values for these plug samples were calculated using equations described in Beaty (*in prep.*). The minipermeameter was also used to measure K_a values for the plug samples and the results were compared with those obtained using the laboratory permeameter. Appendix 3 contains values of K_a that were obtained using these two instruments on plugs from cores T104 P014 and T132 P014.

Thin sections were produced from the material trimmed off of the end of 44 of the plug samples. The locations where plug samples and thin-section samples were extracted from the cores are indicated in Plate 1 and Appendix 1. Thin sections were analyzed using standard petrographic techniques (Williams et al. 1982). Appendix 4 contains the results of thin section analyses of plugs from cores T104 P014 and T132 P014. Parameters that were analyzed in the thin sections included grain size, sphericity, rounding, and sorting. The values of sphericity, rounding, and sorting were estimated using thin section comparison photomicrographs and charts provided by Beard and Weyl (1973). In four areas of each slide, mica, clay and cement percentages were estimated by comparison to charts (Williams et al. 1982). A micrometer scale was used to measure grain sizes in four areas of each slide, and approximately 80 grain size measurements in each slide were averaged (Appendix 4). Because the values of all of these analyses are approximations, they are only used to examine vertical trends.

Results of Analyses

Appendix 1 contains descriptions of the lithology and general sedimentary features of all ten cores. Core descriptions note prominent bounding surfaces, and contain qualitative assessments of mica content and grain size. The results of these macroscopic analyses were similar to the results of thin section estimates of mica content and grain size.

All of the cores were drilled through the South Bend Limestone and contained the lower sequence boundary of the Tonganoxie Sandstone. As in the conglomerate, the lower sequence boundary in the cores directly overlies the Weston Shale (0.08 to 0.33 m (0.25 to 1.00 ft) thick). Lithologic types present in the cores include sandstone consisting of *St* and *Sl* sets, conglomerate, conglomeratic sandstone, and silty sandstone. The cores contain sandstone intervals from the lower and upper flow units described along the outcrop. An interval above the upper flow unit, not present at the outcrop, was observed in the cores. The interval above the upper flow unit generally consisted of *Sl* sets (Miall 1985), horizontal beds, and ripple beds. In the field where the cores were drilled, the uppermost sandstone interval is exposed on the surface. A core drilled in the center of the surface exposure (core T076 P046; Appendix 1) penetrated 1.5 m of sandstone from this uppermost interval.

In the cores, a total of 407 horizontal K_a values were measured in sandstone with less than 5% cement. The measurements were in sandstone from the lower flow unit, the upper flow unit, and the interval above the upper flow unit. Minipermeameter measurements ranged from 51 millidarcies (md) to 3916 md, with a geometric average of 1094 md and an interquartile range (IQR, the range between 25th and 75th percentile of values) of 1157 md. Horizontal K_a values in the lower flow unit ranged from 110 md to 3916 md, with a geometric average of 1310 md and an IQR of 1131 md. In the upper flow unit, horizontal K_a values ranged from 63 md to 3134 md with a geometric average of 1154 md and an IQR of 1475 md. In the interval above the upper flow unit, K_a values ranged from 50 md to 2435 md, with a geometric average of 680 md and an IQR of 504 md.

Both the upper and lower flow units contain varying quantities of muscovite mica (ranging from 0.5 to 8.5 %; Appendix 4), but upper flow unit sandstone sets commonly contain more mica than sets

in lower flow unit sandstone. Thin section estimates of mica content from the upper flow unit yielded values that range from 2.0% to 8.5%, with an arithmetic average of 4.6%. In samples the lower flow unit, mica content ranges from 0.5% to 5.3%, with an arithmetic average of 2.5%.

Vertical K_a measurements, made in the upper and lower flow units along the sandstone outcrop, ranged from 13 to 2100 md, with a geometric average of 833 md (Beaty et al. 1997). Vertical to horizontal K_a (V:H) ratios along the outcrop ranged from 0.18 to 1.0, with an arithmetic average of 0.70. Although horizontal K_a values were similar in the two flow units, vertical K_a values in the upper flow unit were lower than vertical K_a values in the lower flow unit. The lower vertical K_a values in the upper flow unit are attributed to the presence of micaceous lamina boundaries. In upper flow unit sandstone, lamina surfaces were greater than 0.5 mm thick and contained layers of very fine-grained quartz sand, quartz silt, and detrital mica. Mica grains in these layers were at times slightly overlapped. Where mica grains comprised greater than 50% of the volume of the layer, the platy grains formed continuous layers that could significantly affect fluid flow. Vertical permeability measurements perpendicular to these micaceous surfaces were relatively low (<300md) and V:H ratios in these laminated intervals generally ranged from 0.2 to 0.5. Much of the sandstone in the lower flow unit contain lamina surfaces with similar fine-grained, micaceous layers that are generally less than 0.5 mm thick. In many of the lamina, mica grains did not overlap to form continuous layers. However, presence of these layers did affect vertical fluid flow. The V:H ratios through lower flow unit lamina generally ranged from 0.6 to 1.0. Commonly, vertical permeability measurements perpendicular to lamina in the lower flow unit were equal to the corresponding horizontal measurement.

Cross-section Analysis

Cross-sections (Plate 1) were generated using data from core descriptions and wireline logs (Appendix 1), and K_a data (Appendix 2). The cross-sections contain lithologic descriptions of cores and include qualitative assessments of mica, iron oxide or hydroxide, and calcite cement. In addition, graphs of gamma ray, conductivity, and permeability values versus depth are shown. Cross-sections A-

A' and B-B' (Plate 1) depict cores drilled 28 m apart along southeast-trending transects that approximately parallel the local southeast paleo-transport direction (Beaty et al. 1997). Cross-section C-C' (Plate 1) depicts cores drilled 16 m apart along a northeast-trending transect, approximately perpendicular to the local transport direction. Intervals were correlated between cores in the cross-sections using information from core descriptions and wireline logs (Plate 1). In addition, line drawings of the outcrop photomosaic (Figure 3) were compared to correlation lines along cross-section A-A'. Profiles of GPR data from Beaty et al. (1997) were compared to correlation lines along cross-sections B-B' and C-C'. These comparisons made it possible to improve interpretations of the lateral extent of sandstone intervals and infer realistic sandstone geometries at the same scales observed along the outcrop.

Beaty et al. (1997) showed that *S_t* sets analyzed using the GPR grid are commonly less than 10 m (30.5 ft) wide when measured perpendicular to trough axes. It is important to note that at a minimum spacing of 16 m (52.5 ft), the cores were not close enough for correlation lines on the cross-sections to delineate all of the individual scour surfaces between *S_t* sets. Instead, many of the correlation lines, especially those that span the distance of the cross-sections, represent the boundaries between CH intervals that contain groups of *S_t* sets.

In addition to sandstone from the upper and lower flow units, approximately half of the cores also contained very fine-grained micaceous sandstone and silty sandstone from an interval above the upper flow unit. In comparison to sandstone in the upper and lower flow units, the uppermost sandstone interval contained a greater percentage of silt-sized quartz grains, generally contained greater than 6% mica and greater than 5% mud (detrital clay minerals), and exhibited lower horizontal K_a values. Some of the plane beds and *S_t* sets contained alternating thick and thin lamina and the ripple beds contained mud-draped reactivation surfaces. These beds extended throughout the GPR grid of Beaty et al. (1997), and could be correlated through cores in cross-sections B-B' and C-C' (Plate 1).

Many of the cores contained a basal conglomerate and conglomeratic sandstone interval similar to the one described earlier (p. 3). However, unlike that outcrop, conglomerate was not always the most

abundant lithologic type in this basal interval. The basal conglomerate and conglomeratic sandstone interval in cores varied in lateral thickness and contained clasts of varying sizes. Clast abundance generally ranged from 20% to 50%, although a few beds contained up to 70% clasts. Cross-section C-C' shows that the basal conglomerate and conglomeratic sandstone interval has an undulating upper boundary. In most of the cores, the basal interval contains thin conglomerate beds (less than 15 cm) with 2 mm to 10 mm clasts. Most conglomerate beds could not be correlated between cores. Only three of the cores in cross-section C-C' contained beds with significant clast concentrations in the lower 15 cm (0.5 ft) of the interval, just above the sequence boundary.

Along the sandstone outcrop, a few thin, laterally discontinuous, conglomeratic sandstone beds were present at the base of trough scours. These types of thin conglomeratic sandstone beds were also observed in many of the cores. Like basal conglomerates, conglomeratic beds at higher levels in the fluvial succession were extremely variable in thickness along the scour surface and clast abundance ranges from 20% to 50 %. In outcrop, upper conglomerates and conglomeratic sandstones were much more limited in extent (less than 3 m (9.8 ft)) than the basal conglomerates in the outcrop across the highway.

Thin Section Analysis

Analysis of thin sections (Appendix 4) revealed that quartz grain size in the sandstone cores ranged from 0.09 mm (very fine-grained) to 0.17 mm (fine-grained). Beard and Weyl (1973) point out that thin section measurements of grain size tend to underestimate the actual grain size of samples. However, the results of the thin section grain size estimates are consistent with grain size sieve analyses performed on four *S_t* samples near the study site (Minor 1969). The thin section grain size measurements were sufficient to analyze vertical trends in grain size variation.

The thin sections contained subangular to subrounded and moderately sorted to very well sorted quartz grains (Appendix 4). Estimated mica content in the samples ranged from 0.5% to 8.5%, and averaged 2.5%. Estimated clay content in the samples ranged from 0.50% to 8.00% and averaged

3.4%. The highest amounts of clay were observed in samples containing shale clasts. Cements consisted of iron oxide and hydroxide in the upper portions of the cores and calcite and iron oxide and hydroxide cement in lower portions of the cores. Samples from intervals in the upper portions of the cores contained 2.0% to 5.0% iron oxide or hydroxide cement, and measured K_a values in these samples were generally greater than 1200 md. Measurements of K_a in calcite-cemented intervals near the base of the core commonly yielded values that were less than 1 md.

Wireline Log Analysis

Sandstone in the lower flow unit generally produces gamma ray intensity in the range of 40 to 70 counts per second (cps). Gamma ray values fluctuate with respect to position within *St* sets. As shown in the detailed core descriptions (Appendix 1), mica was a common constituent in these rocks. The magnitudes of gamma ray and conductivity values from the wireline logs corresponded roughly to qualitative assessments of mica and mud content observed in cores and in thin sections.

The conductivity and gamma ray logs provided information concerning the location of bounding surfaces. Intervals in the logs containing relatively small increases in conductivity (3-5 milli-Siemens/meter (mS/m) for 6-12 cm intervals) and shifts in gamma ray intensity (to values greater than 60 cps) corresponded to mica-rich bounding surfaces observed in core.

Core holes containing the upper flow unit had high gamma ray values. Core descriptions and thin section analyses demonstrated that this interval contained more mica, silt, and mud than sandstone from the lower flow unit. In the cores, the silty sandstone in the interval above the upper flow unit generally contains the most mica and generally exhibited the highest gamma ray values. Several of the core descriptions in Appendix I describe sandstone from this interval and the cross-sections in Plate 1 show that the lower contact of the interval is relatively flat.

Iron-rich zones (Fe oxides and hydroxides) identified in cores commonly exhibited conductivity values 10-20 mS/m higher than uncemented zones, while gamma ray values remained unchanged from those in uncemented zones. As iron-rich zones commonly have relatively low permeability values (<10

millidarcies (md)) and cause signal attenuation in GPR data (Martinez et al., *in review*), these findings have implications for evaluating the suitability of sites for near-surface GPR studies where wells logs are available but cores are not.

Comparison of K_a Measurement Techniques

In order to compare K_a values measured using minipermeameter and laboratory permeameter analyses, 36 core plugs from cores T132 P014 and T104 P014 were analyzed (Appendix 5). Appendix 5 contains the results of conventional statistical analyses of K_a and porosity values from laboratory analyses and K_a values from minipermeameter analyses.

Regression analyses comparing the results of the two measurement methods produced an R^2 value of 0.94, a slope of 1.07, and an intercept of -29.5 suggesting that the two measurement techniques yield comparable K_a values (Figure 5, Appendix 6). In Figure 5, values are scattered almost equally on either side of a regression line plotted diagonally on the graph. This observation suggests that there is no systematic bias imparted to K_a values obtained using either measurement method (Davis 1986). In the 26 plug samples containing less than 5% cement, the geometric averages of K_a measurements was 1538 md for laboratory analyses and 1561 md for minipermeameter analyses. The plug samples had an average porosity of 34.1%.

Discussion

With a minimum separation distance of 16 m across the direction of transport (cores along cross-section C-C'), CH intervals can be correlated between wells. The correlations provide a framework within which to analyze lateral variations in lithologic types and permeability values. However, the cores are not spaced closely enough to determine the lateral continuity of many of the *St* sets. The lateral continuity of these *St* sets can be better defined using GPR data to obtain a relatively continuous sampling between cores (Martinez et al. 1998). A study by Martinez (*in prep.*) analyzes vertical profiles of 225-Megahertz (MHz) GPR data that parallel the cross-sections in Plate 1. These GPR

profiles provide the close data spacing that is needed to image the bounding surfaces between these cross-bed sets.

The difficulty in correlating sandstone horizons between wells using only the data obtained from the cores made it necessary to compare the photomosaic (Figure 3) and GPR profiles from Beaty et al. (1997) with cross-sections (Plate 1). By making these comparisons it was possible to correlate intervals between cores and impart the types of geometry observed along the outcrop. An example of the results obtained by such comparison is shown in cross-section C-C' (Plate 1). By projecting a northeast-trending profile from the GPR grid, it was possible to identify the location of a large channel discussed in Beaty et al. (1997). A green line on Cross-section C-C' highlights the location of the base of this channel.

The magnitudes of permeability values within adjacent scour-channel fills are often different, but the general permeability architecture of the channel fills is similar. The lowest permeability sandstone (50 to 400 md) occurs near the base of channel fills and permeability values generally increase upward. In sandstone samples from the lower flow unit, an inverse relationship was observed between mica content and horizontal K_a values. Gamma-ray values generally decreased upward within individual *St* sets in the lower flow unit. In the *St* sets containing less than 5% cement, K_a values generally increase upward. Many of the intervals in the lower flow unit (Plate 1) contain this upward trend in K_a values. Analyses of petrologic characteristics of *St* sets along the sandstone outcrop and in cores, reveal that lamina from areas near the basal scour surfaces of sets tend to contain more platy mica than lamina higher in the set. The observed upward increase in K_a values was also observed during a small-scale study of *St* sets discussed in Beaty et al. (*in prep.*). A few intervals contain several such upward trends in K_a values as they likely contain several cross-cutting *St* sets.

The cores contain conglomeratic beds that occur at different stratigraphic levels and do not extend between cores. Conglomerate beds at all stratigraphic intervals are similar in composition and tend to contain mostly rounded shale lithoclasts with minor angular limestone fragments. Beds containing thick (greater than 15 cm) shale- and limestone-clast conglomerate are not always present at the base

of the cores (Appendix 1 and Plate 1) suggesting that the conglomeratic interval is sporadic in distribution.

Interpretations

In the lower flow unit, *S_t* sets generally trend toward the southeast whereas in the upper flow unit, many *S_t* sets trend toward the southwest, especially near the top of the unit (Beaty et al. 1997). This change in the orientation of *S_t* sets suggests that the local sediment transport direction changed through time. Near the top of the cored interval, increased gamma ray values are likely due to the increased mica and mud content. Horizontal K_v values in this interval are lower than the other sandstone intervals (Plate 1). In many of the cores, silty and micaceous plane beds and *S_t* sets from the interval above the upper flow unit contain alternating thick and thin sandstone lamina, suggesting that the sandstone was deposited in an estuary. The presence of mud draped reactivation surfaces and ripple crests in this uppermost interval reinforces the interpretation of an estuarine origin for this uppermost interval.

In the lower flow unit, individual lamina contain quartz sand that is remarkably uniform in grain size but contain differing percentages of mica, depending on position within the *S_t* set. Observations of sandstone in *S_t* sets along the outcrop and the upward decrease in gamma ray values in *S_t* sets in core suggest that during dune migrations within trough scours, finer grained and platy material was concentrated at the toe of foreset beds. The presence of mica causes some basal sandstone lamina to have lower vertical K_v values, inhibiting hydraulic communication between cross-cutting troughs (Beaty et al., *in prep.*). Values of V:H ratios across these bounding surfaces range from 0.6 to 1.0, with the lowest values near the base of the trough scour and the highest values in lamina at the margins of the trough scour (Beaty et al., *in prep.*). Along the outcrop, bounding surfaces between lamina at the margins of scour-channel fills are commonly barely perceptible. Thus, lamina boundaries in these marginal areas of the trough would likely be negligible barriers to fluid flow. Conversely, because of their lower V:H ratios, the presence of micaceous sandstone lamina at the bases of trough scours may

have a more marked effect on fluid flow (Beaty et al., *in prep.*). Micaceous sandstone lamina at the bases of trough scours account for only a small percentage of the volume of sandstone, but they are one of the most important controls on the permeability architecture of systems containing fluvial *Sf* sets (Weber 1982).

Mica content was not the only factor that influenced the magnitude of horizontal K_a values. Magnitudes of horizontal K_a values were also influenced by other parameters such as the grain size, the degree of sorting, and the amount of iron oxide or hydroxide cement present. Beard and Weyl (1973) suggest that grain size and sorting are the two most important controls on the permeability values of sandstone. Minipermeameter and laboratory permeameter measurements of K_a values in sandstone containing thick sandy lamina with little mica are similar to permeability values measured for wet-packed sandstone with similar grain sizes and degrees of sorting (Beard and Weyl 1973). In samples with relatively little cement, micaceous lamina boundaries are the most likely cause of dissimilarities between Tonganoxie Sandstone and Beard and Weyl (1973) values. Thin section analyses reveal that samples containing >4% mica generally have significantly lower horizontal K_a values than samples containing thick sandy lamina with little mica, even when they contain quartz sand with similar grain size and sorting (Appendix 4).

In incised valley-fills, conglomerate is generally thought to develop in fluvial valleys as a lag deposit on the sequence boundary during eustatic lowstand (Zaitlin et al. 1994) or as a lag deposit along ravinement surfaces during transgression (Van Wagoner 1990). The basal interval in most of the cores did not contain as much conglomeratic material as the beds in the conglomerate outcrop (p. 3) across the road from the sandstone outcrop. Observing the thickness and extent of conglomerate and conglomeratic sandstone beds only along the outcrop could easily cause the investigator to infer that they are of significant lateral extent. However, it was not possible to correlate even the thicker conglomeratic beds between closely spaced core holes. The presence of conglomeratic sandstone beds that occur sporadically, at higher levels in the cores suggests that clast developments were not limited to lag deposits associated with unique chronostratigraphic surfaces. Such rapid changes suggest that

autogenic processes may be responsible for distributing the conglomeratic material. The conglomerate clasts may have come from nearby tributary valleys during times of downcutting and headward erosion (Beaty, *in prep.*).

The observation that conductivity logs responded to changes in mica content is important for interpretation of ground-penetrating radar (GPR) data. The micaceous surfaces have increased conductivity resulting in attenuation of radar signals. As a result, these micaceous surfaces usually are good electromagnetic reflectors. Caution must be used when interpreting conductivity logs in wells without cores, however, because not all such perturbations are related to changes in mica content. Conductivity values can also increase in the presence of iron oxide and hydroxide cements. Fe oxide and hydroxide cements are highly conductive and absorb much of the GPR signal, causing attenuation.

Conclusions

At the fluvial study site, studies of cross-cutting *St* sandstone sets along the outcrop face yielded two-dimensional information concerning the variability of lithologic types and distribution of K_a values, but revealed little concerning their three-dimensional variability. Closely spaced cores from behind the outcrop face allowed the distribution of lithologic types to be studied in three dimensions and allowed laboratory analyses of K_a , porosity, and grain density.

By comparing the cross-sections with the photomosaic and GPR profiles, it was possible to incorporate realistic geometric information to all CH intervals and correlate intervals with disparate well log and core information. In many cases, CH intervals were correlative across entire core cross-sections. Although it was not possible to correlate many of the individual *St* sets between cores, the cores provided very important information concerning vertical variations in lithologic types, permeability values, and well log response through the sets.

The magnitudes of the K_a values between vertically adjacent sets are commonly different, but the general K_a architecture of the *St* sets are very similar. In cores and in outcrop, an inverse relationship was observed between mica content and horizontal K_a values. Along individual lamina, quartz sand

was remarkably uniform in grain size. In vertical profile, lamina contained differing percentages of mica, depending on position within the *S_t* set. Platy material was concentrated at the toe of foreset beds during dune migrations within trough scours. The presence of greater percentages of mica in the lowest portions of trough scours may inhibit hydraulic communication between *S_t* sets in these areas.

Conglomeratic intervals in cores were not as well developed as those observed across the road from the fluvial outcrop site of Beaty et al. (1997) and conglomeratic sandstone also occurs at higher intervals in many of the cores. These findings suggest that autogenic processes dominated the deposition of the conglomerate beds. The conglomeratic intervals are not exclusively lag deposits associated with unique chronostratigraphic surfaces related to different phases of relative sea level change.

Permeability values measured with the minipermeameter and lab permeameter yielded comparable results. A statistical comparison of K_a measurements found that no significant difference exists between the values obtained using the two techniques.

Wireline logs were used to analyze the causes of reflections and signal attenuation in GPR data obtained from the field. Micaceous lamina surfaces cause minor increases in conductivity and, thus, act as electromagnetic reflectors. Conversely, iron oxide cements are highly conductive and absorb much of the GPR signal causing attenuation.

Acknowledgements

We would like to thank Joe Anderson, who providing drilling and coring services for this project, and David Young, who performed the wireline logging. Frank and Virginia Gray graciously allowed land access and provided drilling permission. Alan Byrnes provided assistance with laboratory permeability and porosity analysis. Colin Robins assisted with minipermeameter analyses and drafting of the figures for this report. Tim Carr edited the final manuscript and provided helpful suggestions. Special thanks go to Tony Walton from the Geology Department of the University of Kansas for editing an early, very rough version of this paper.

References

- Archer, A. W., H. R. Feldman, and W. P. Lanier, 1993, Road log and field guide, *in* A. W. Archer, H. R. Feldman, and W. P. Lanier, eds., *Incised paleovalleys of the Douglas Group in northeastern Kansas: field guide and related contributions*, Kansas Geological Survey Open-File Report 93-24, Stop 1-3.
- Archer, A. P., W. P. Lanier, and H. R. Feldman, 1994, Stratigraphy and depositional history within incised-paleovalley fills and related facies, Douglas Group (Missourian/Virgilian; Upper Carboniferous) of Kansas, U. S. A., *in* R. W. Dalrymple, R. Boyd, and B. A. Zaitlin, eds., *Incised Valley Systems: Origin and Sedimentary Sequences*: SEPM (Society for Sedimentary Geology) Special Publication No. 51, p. 175-190.
- Beard and Weyl, 1973, Influence of texture on porosity and permeability of unconsolidated sand: *American Association of Petroleum Geologists Bulletin*, V. 57, No. 2, pp. 349-369.
- Beaty, D. S., *in prep.*, Stratigraphic influences on the permeability architecture of fluvial and estuarine sandstones in the Tonganoxie incised valley-fill of northeast Kansas, USA. Ph.D. dissertation, University of Kansas.
- Beaty, D. S., A. Martinez, and A. Byrnes, *in prep.*, Permeability structure and fluid-flow characteristics of fluvial trough cross-beds, Tonganoxie sandstone, northeast Kansas: SPE Formation Evaluation.
- Beaty, D. S., A. Martinez, and A. W. Walton, 1997, Combined minipermeameter and ground-penetrating radar characterization of Tonganoxie valley-fill sandstones, Upper Pennsylvanian, northeastern Kansas, *in* *Shallow Marine and Nonmarine Reservoirs; Sequence Stratigraphy, Reservoir Architecture, and Production Characteristics*. Proceedings of the Gulf Coast Section Society of Economic Paleontologists and Mineralogists, 18th Annual Research Conference, Houston, Texas, December 1997, p. 47-63.
- Davis, J. C., 1986, *Statistics and Data Analysis in Geology*: John Wiley and Sons, New York, 646 p.
- Feldman, H. R., M. R. Gibling, A. W. Archer, W. G. Wightman, and W. P. Lanier, 1995, Stratigraphic architecture of the Tonganoxie paleovalley fill (Lower Virgilian) in Northeastern Kansas: *AAPG Bulletin*, v. 79, p. 1019-1042.
- Martinez, A., *in prep.*, Ground-penetrating radar in sedimentary rocks of northeast Kansas, USA. Ph.D. dissertation, University of Kansas.
- Martinez, A., and D. S. Beaty, *in review*, Stratigraphic imaging capabilities of ground-penetrating radar in a fluvial sandstone: *Geophysics*.
- Martinez, A., E. K. Franseen, and D. S. Beaty 1998. Applications of ground-penetrating radar to sedimentologic and stratigraphic studies - examples from Pennsylvanian siliciclastics and carbonates in Kansas: GPR 98 conference expanded abstract, 6 p.
- Miall, A. D., 1985, Architectural-element analysis: a new method of facies analysis applied to fluvial deposits: *Earth Science Reviews*, v. 22, p. 261-308.

- Minor, J. A., 1969, Petrology of the Tonganoxie Sandstone (Pennsylvanian), Kansas-Missouri: MS thesis, University of Missouri, Columbia, Missouri, 98 p.
- O'Conner, H. G., 1960. Geology and ground water resources of Douglas County, Kansas: Kansas Geological Survey Bulletin 148, 200 pp.
- Weber, K. J., 1982, Influence of common sedimentary structures on fluid flow in reservoir models: *Journal of Petroleum Technology*, V. 34, No. 3, p. 665-672.
- Williams, H., F. J. Turner, and C. M. Gilbert, 1982, *Petrography: an introduction to the study of rocks in thin sections*; second edition. W. H. Freeman and Company, New York, 626 pp.
- Zaitlin, B. A., R. W. Dalrymple, and R. Boyd, 1994, The stratigraphic organization of incised-valley systems associated with relative sea-level change, *in* R. W. Dalrymple, R. Boyd, and B. A. Zaitlin, eds., *Incised valley systems: origin and sedimentary sequences*: SEPM Special Publication 51, p. 45-60.

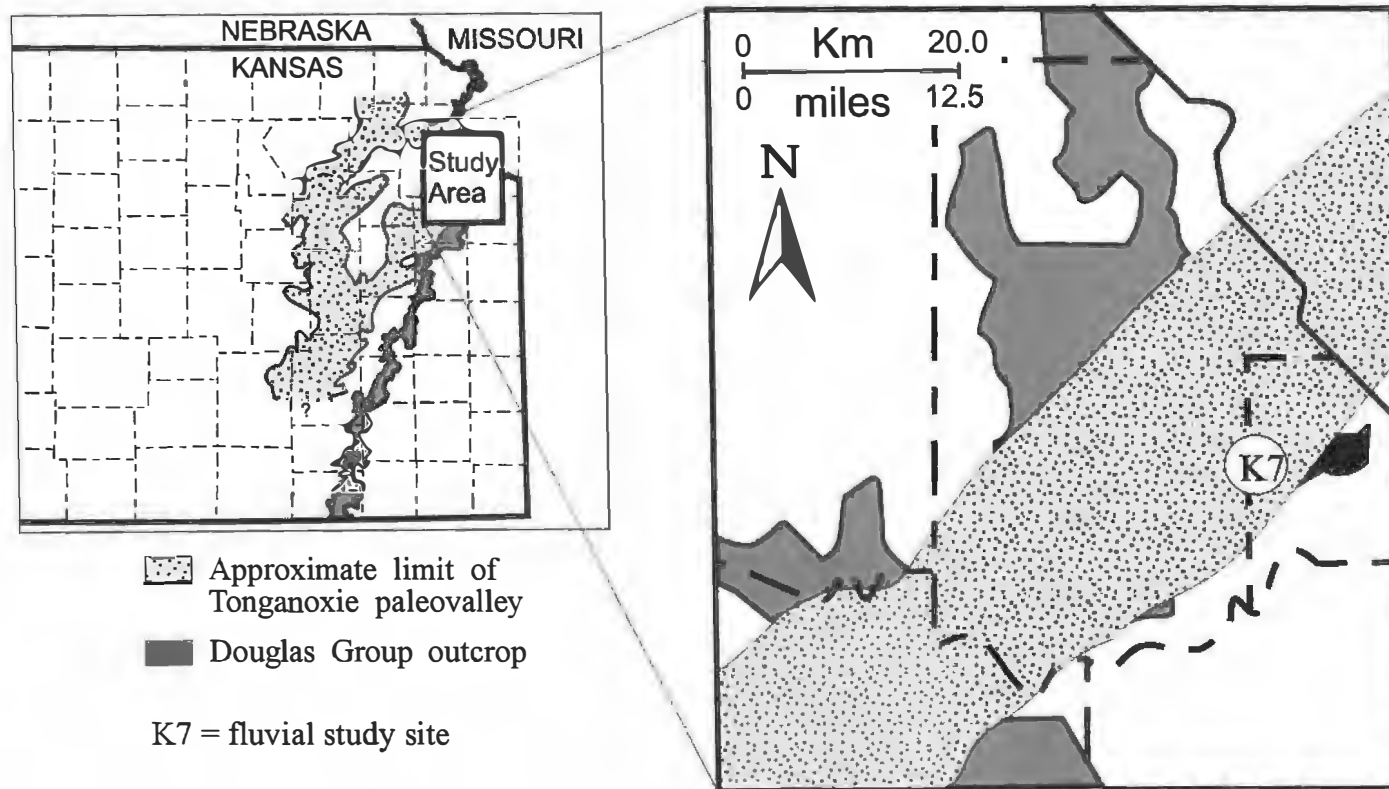


Figure 1 - Maps showing the location of the fluvial study site in northeast Kansas in relation to the limits of the Tonganoxie Paleovalley and the outcrop belt. Modified from Feldman et al. (1995).

(From Feldman et al., 1995)

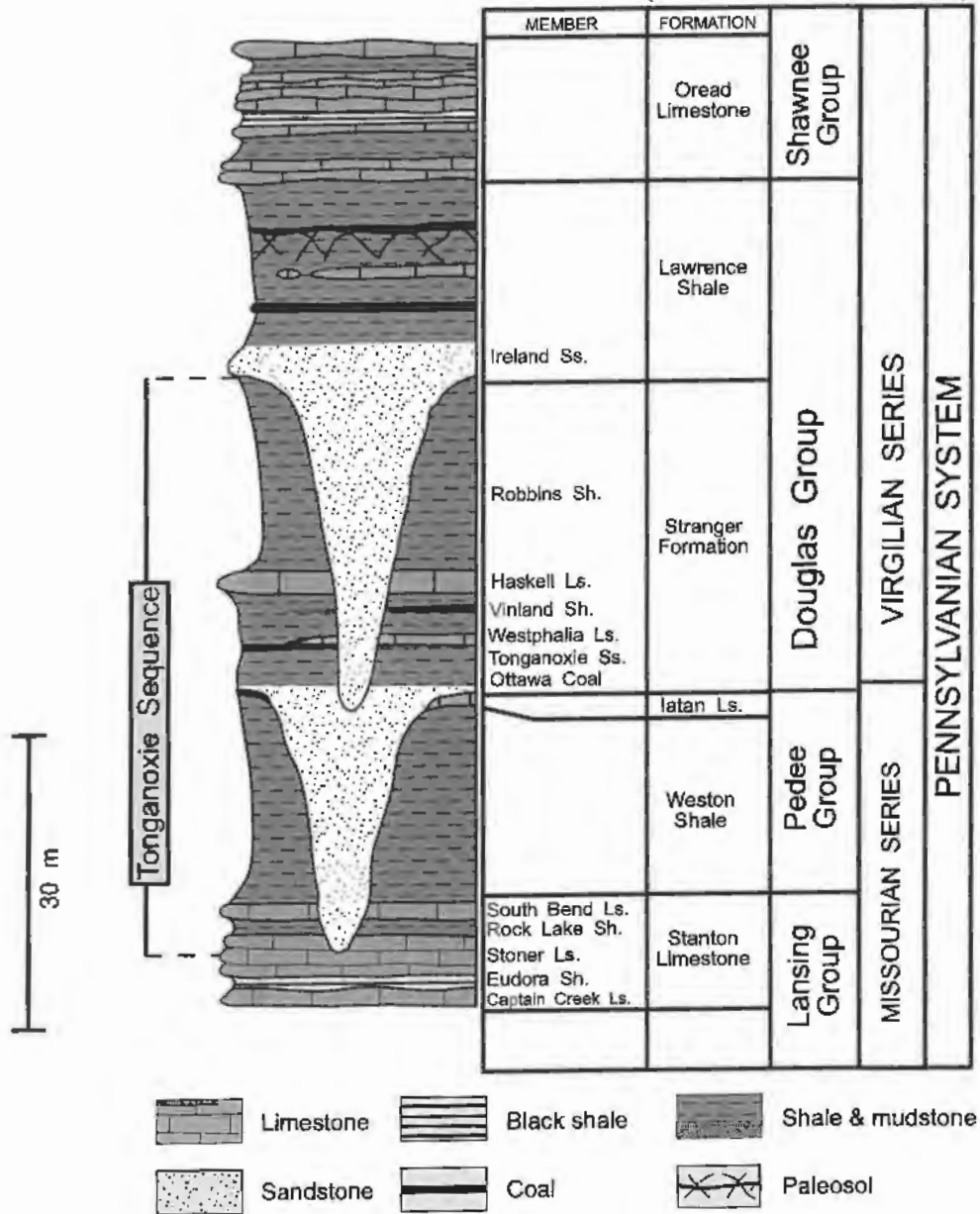


Figure 2 - Stratigraphic chart showing the placement of the Tonganoxie IVF in the Pennsylvanian System. The lower and upper boundaries of the Tonganoxie Sequence (Archer et al. 1994) are shown on the left side of the diagram. Modified from Feldman et al. (1995).

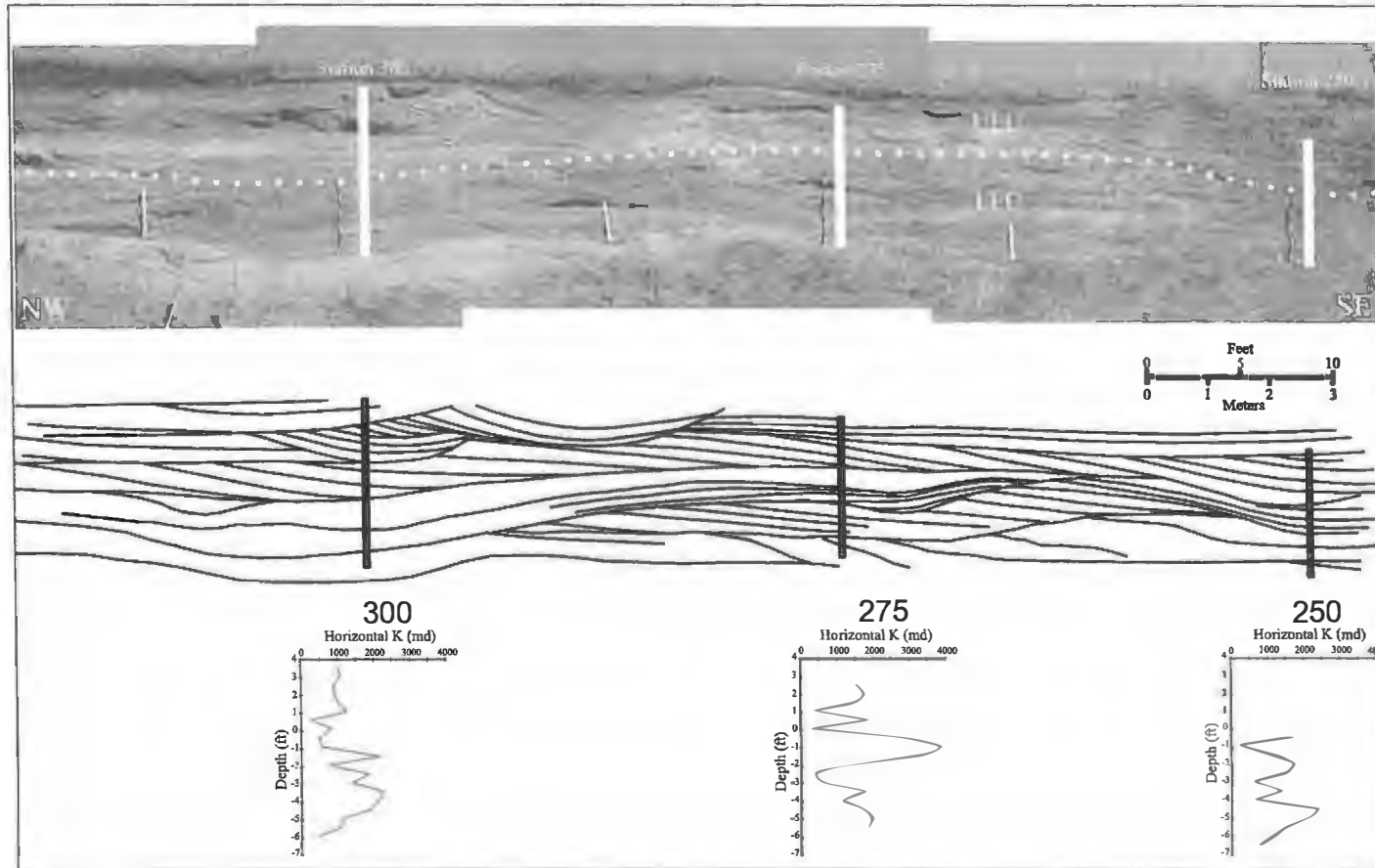


Figure 3 - Photomosaic showing a 25 m (82 ft) long segment of the outcrop at the Highway 7 Fluvial Study site in Wyandotte County, Kansas. The vertical white lines on the photomosaic show the locations of the horizontal K profiles at the bottom of the diagram. The dashed white line shows the approximate location of the boundary between the upper flow unit (UFU) and the lower flow unit (LFU).

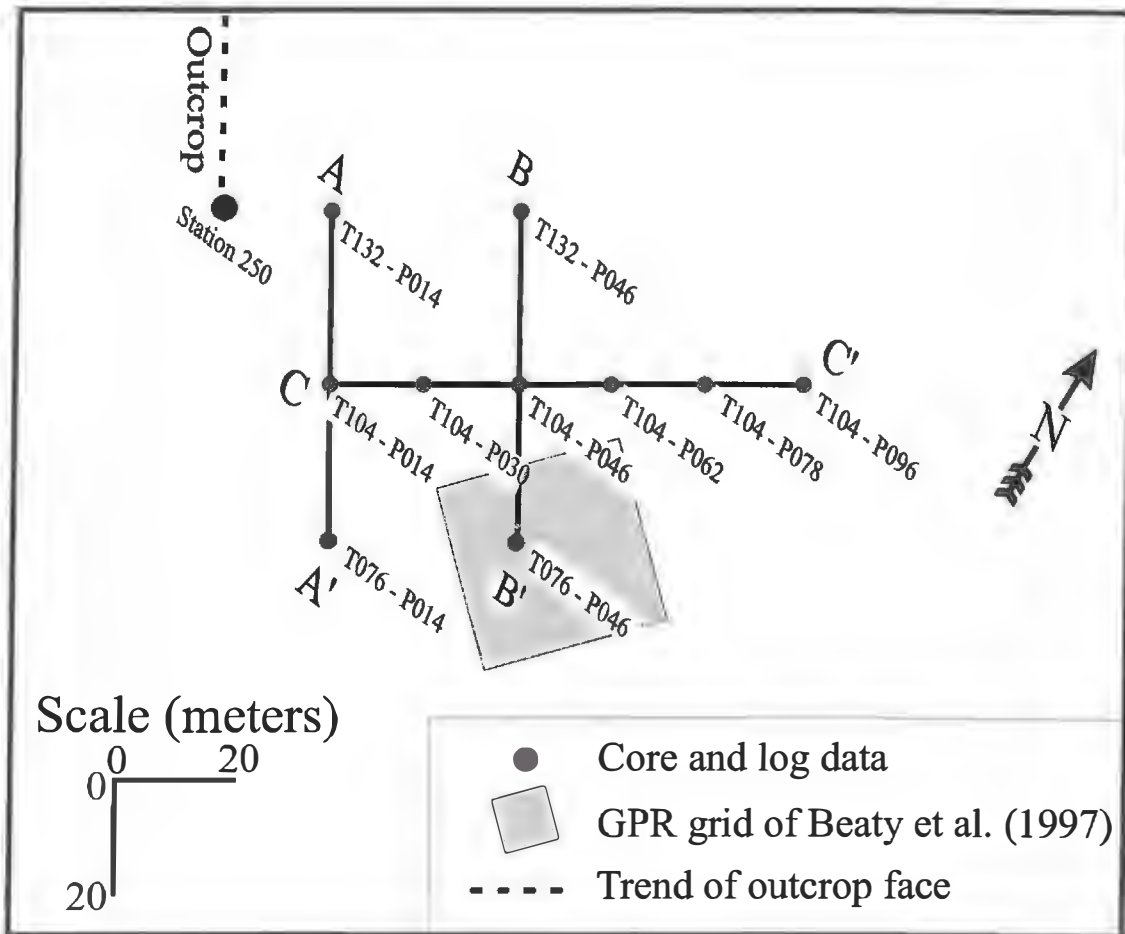


Figure 4 - Location of cores examined in this study. 10 cores were drilled in the field behind the fluvial outcrop site of Beaty et al. (1997). Six of the cores were drilled 16 meters apart in a northeast-trending transect and four were drilled 28 meters away from the transect. Core T132 P014 was drilled approximately 18 meters from the outcrop face, northeast of station 250.

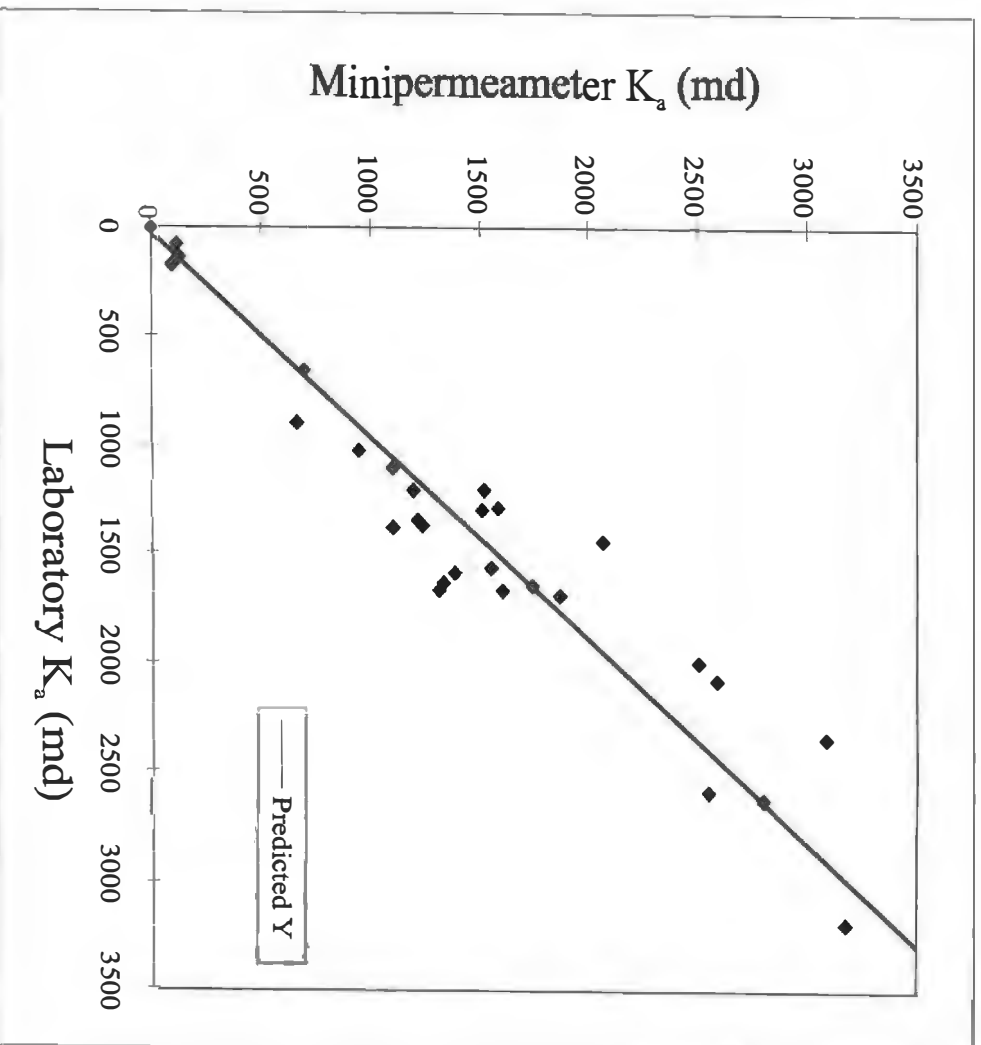




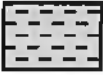


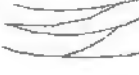

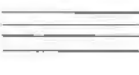





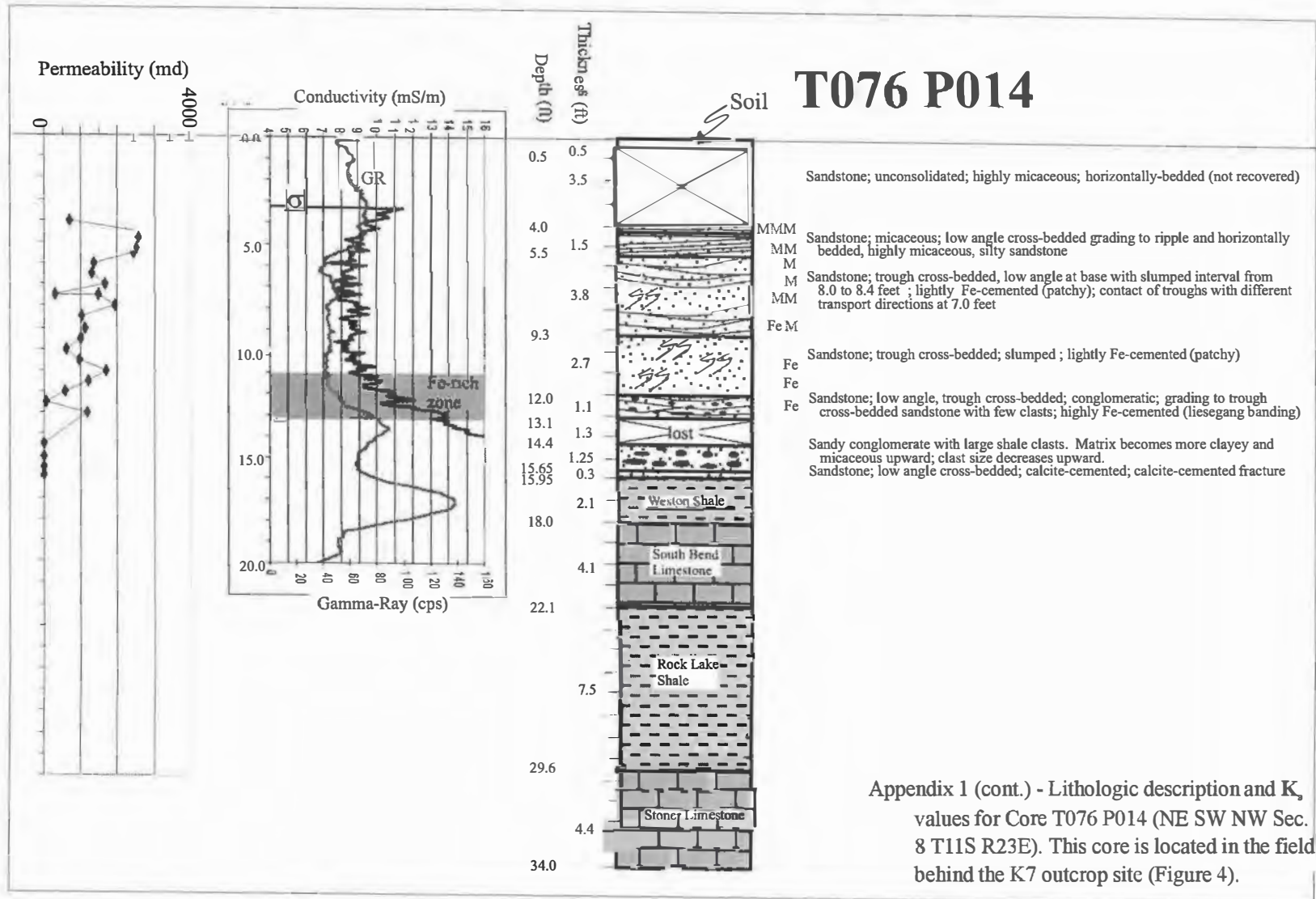
Figure 5 - Comparison of minipermeameter and laboratory air permeability (K_a) values for 36 plugs from cores T104 P014 and T132 P014.

Legend

	sandstone		slumped strata
	limestone		muddy sandstone
	shale		ripple bedding
	interval not recovered	M	2 - 4 % mica
	trough cross-bedding	MM	4 - 6% mica
	low angle cross-bedding	MMM	>6% mica
	horizontal beds	Cc	- calcite cement
	conglomeratic clasts	Fe	- iron oxide cement
			- K _a measurement (laboratory)
			- K _a measurement (minipermeameter)
		TS	- thin section

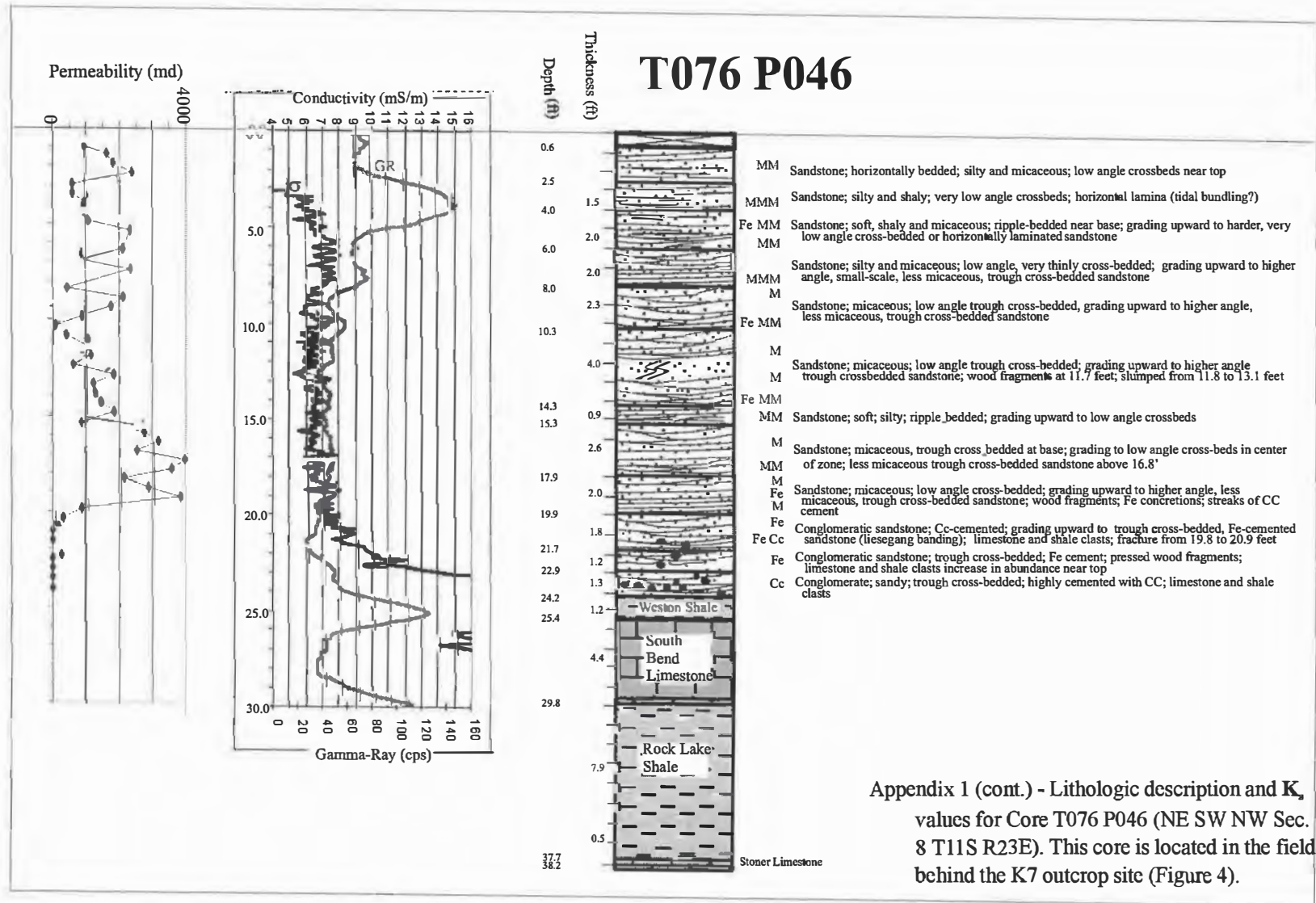
Appendix 1 - Legend for descriptions of 10 cores from Wyandotte County, NE
SW NW Section 8, Township 11 South, Range 23 East.

T076 P014

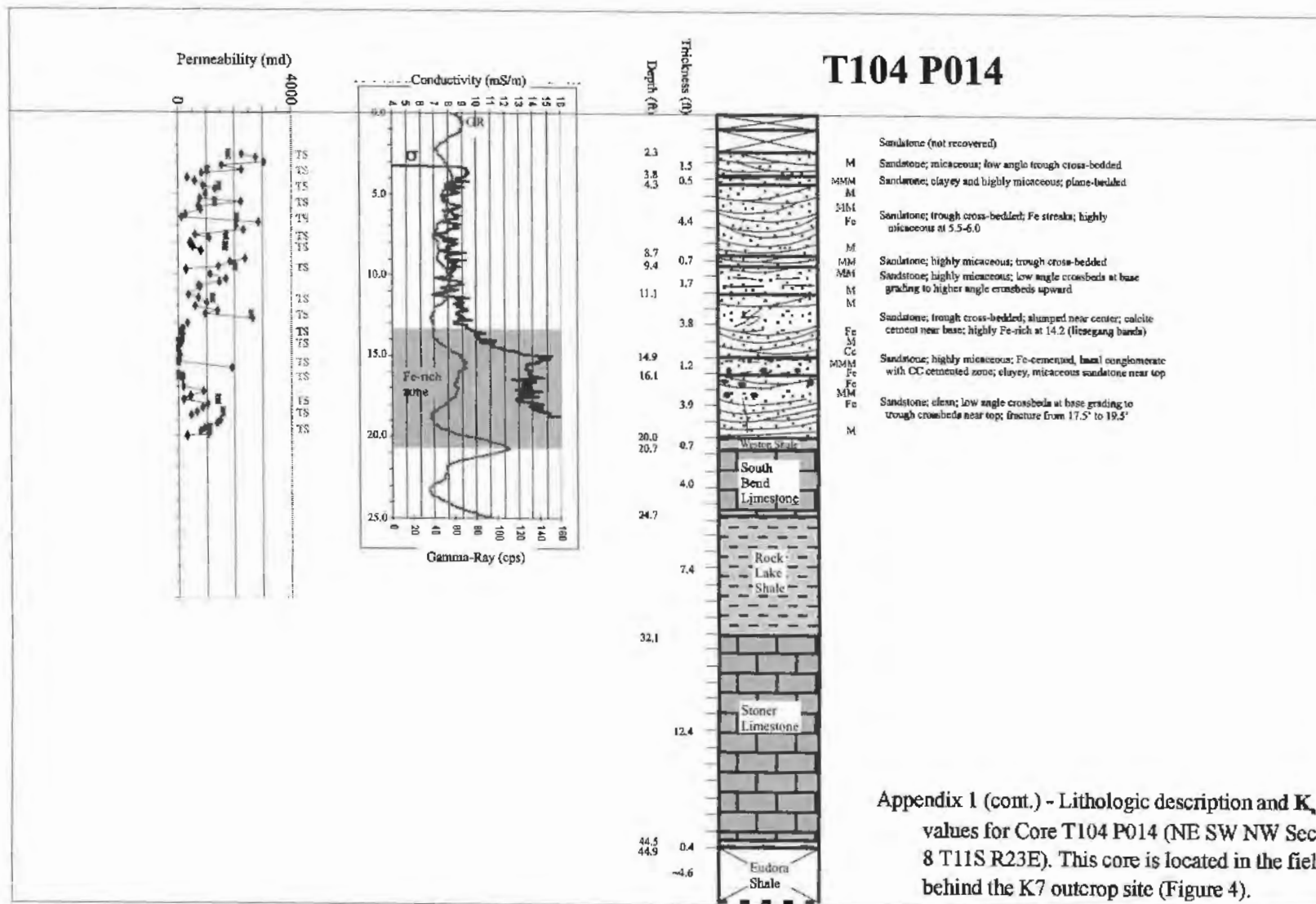


Appendix 1 (cont.) - Lithologic description and K_v values for Core T076 P014 (NE SW NW Sec. 8 T11S R23E). This core is located in the field behind the K7 outcrop site (Figure 4).

T076 P046

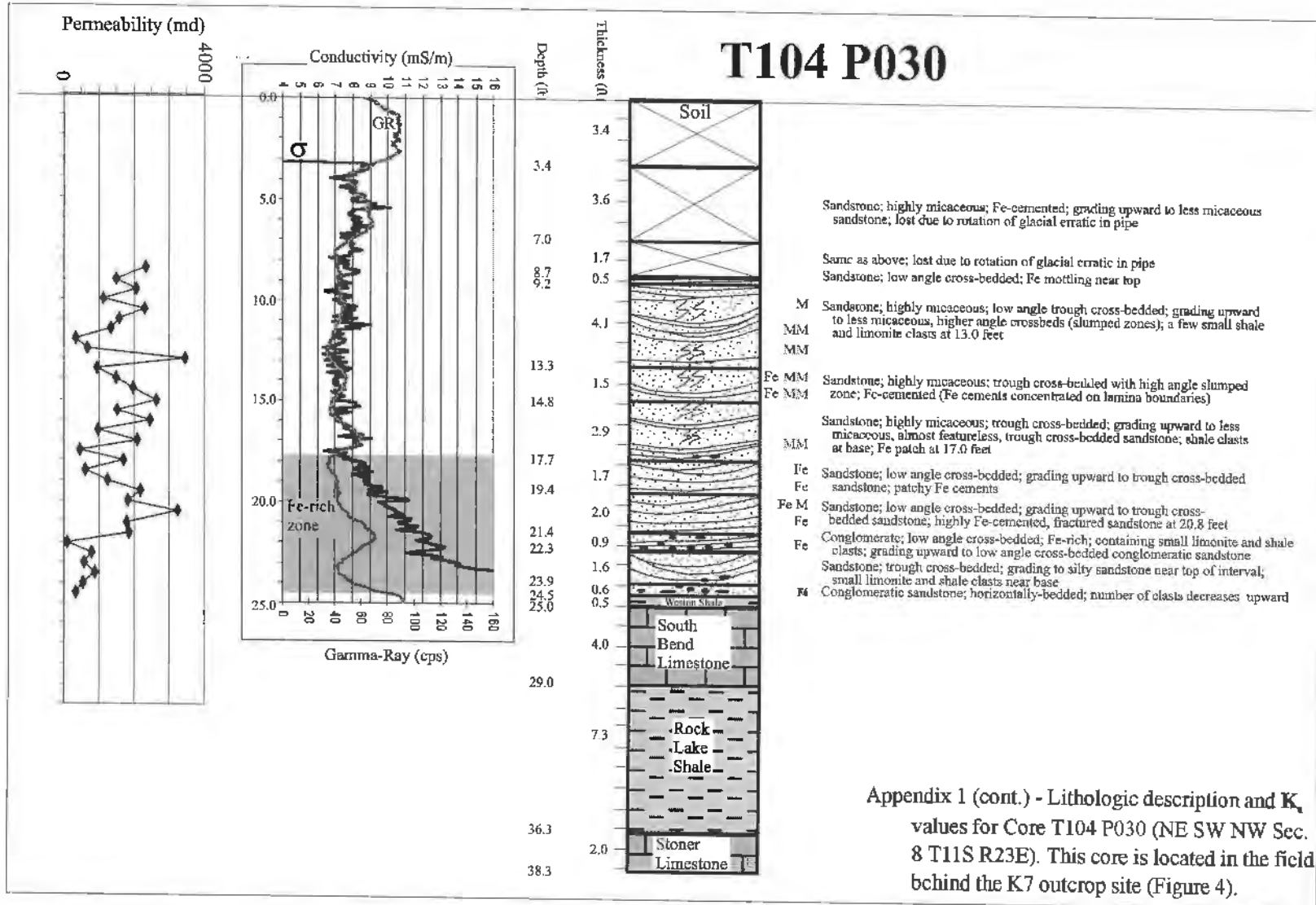


Appendix 1 (cont.) - Lithologic description and K_v values for Core T076 P046 (NE SW NW Sec. 8 T11S R23E). This core is located in the field behind the K7 outcrop site (Figure 4).

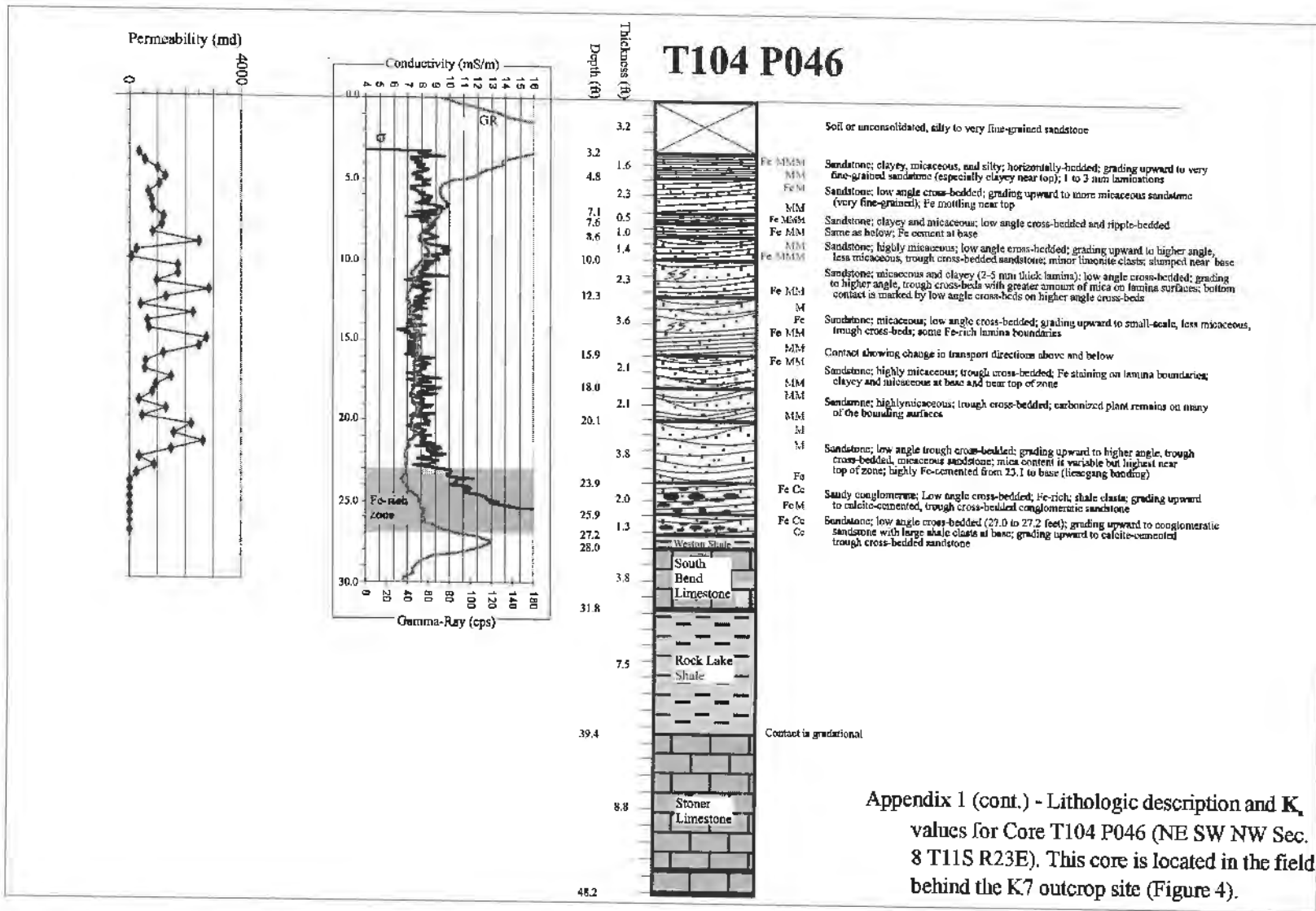


Appendix 1 (cont.) - Lithologic description and K_v values for Core T104 P014 (NE SW NW Sec. 8 T11S R23E). This core is located in the field behind the K7 outcrop site (Figure 4).

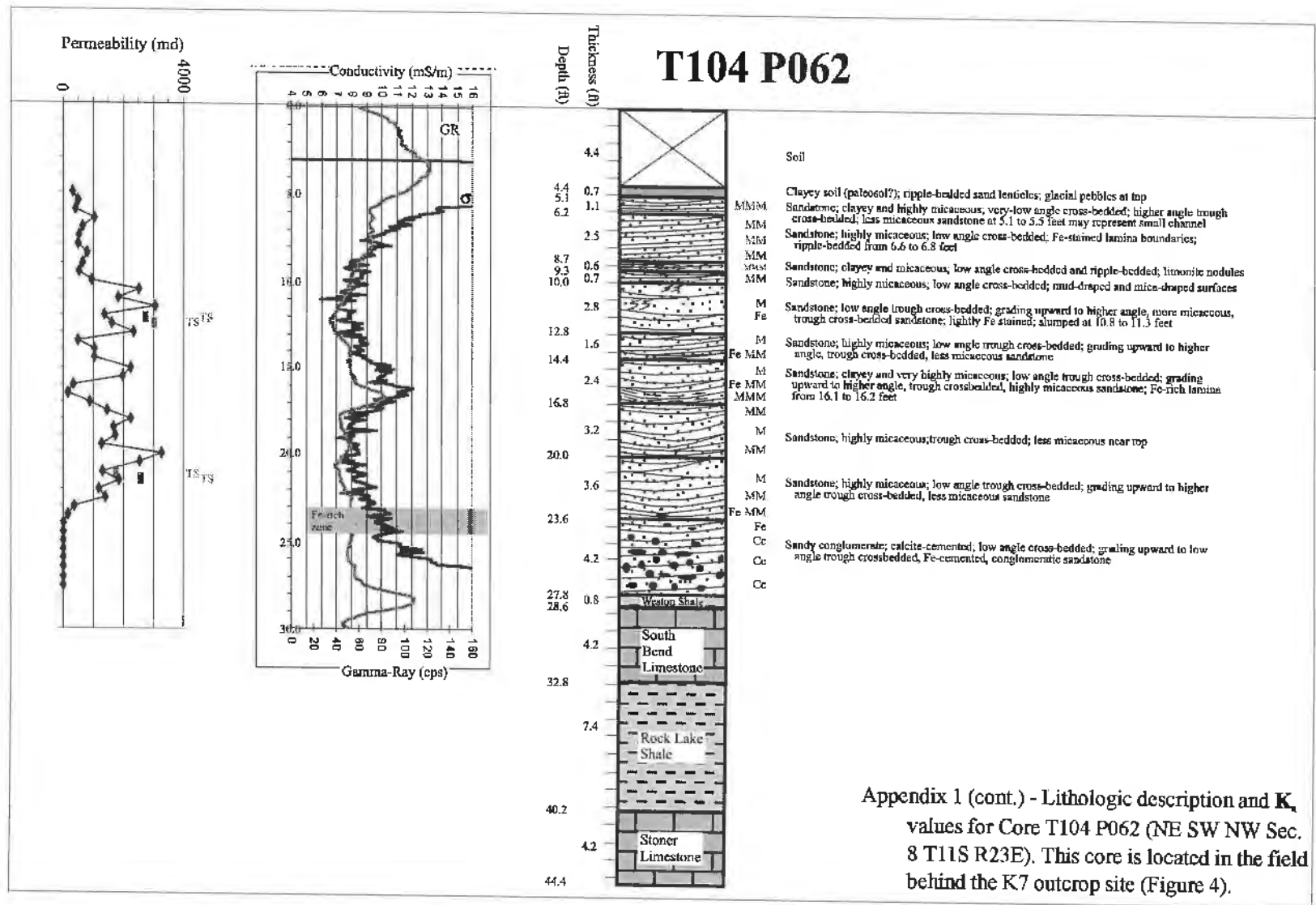
T104 P030

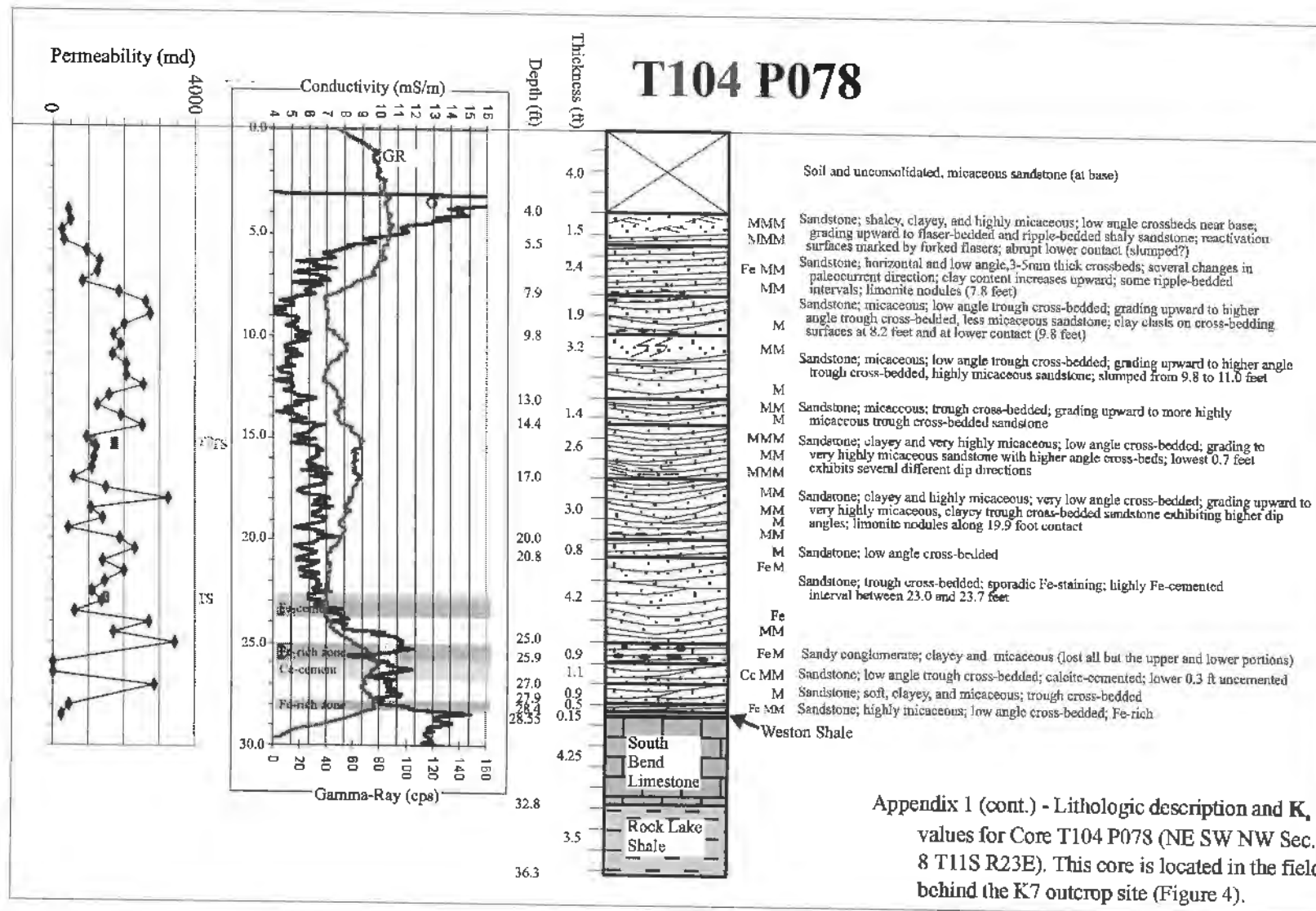


Appendix 1 (cont.) - Lithologic description and K_f values for Core T104 P030 (NE SW NW Sec. 8 T11S R23E). This core is located in the field behind the K7 outcrop site (Figure 4).

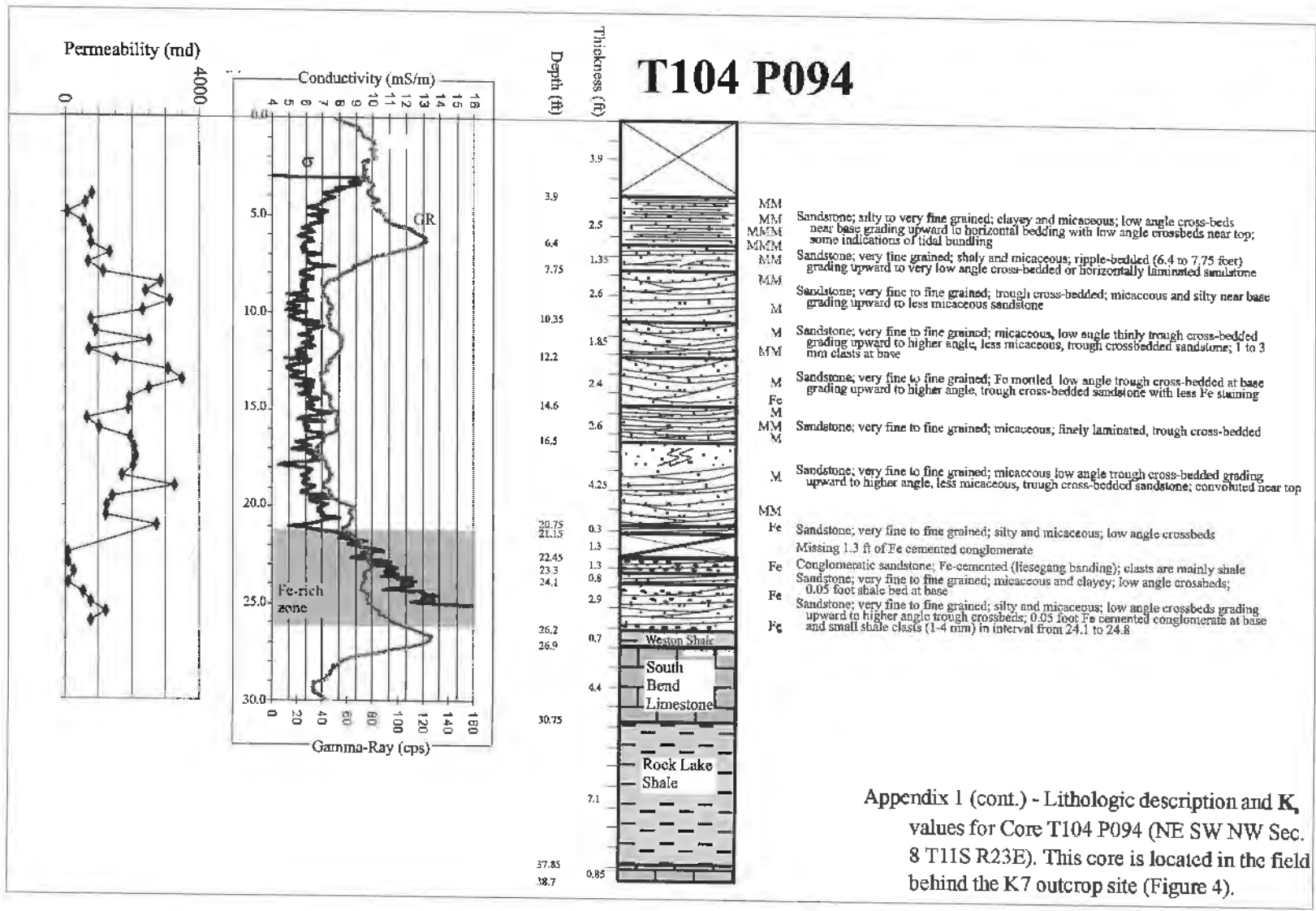


Appendix 1 (cont.) - Lithologic description and K_f values for Core T104 P046 (NE SW NW Sec. 8 T11S R23E). This core is located in the field behind the K7 outcrop site (Figure 4).





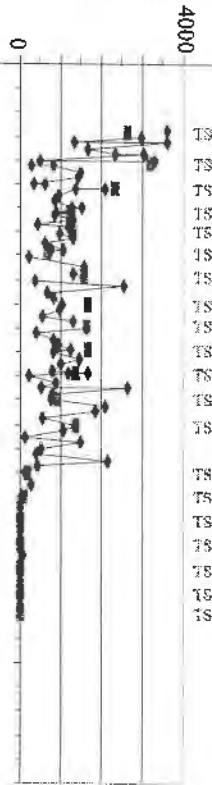
Appendix 1 (cont.) - Lithologic description and K_v values for Core T104 P078 (NE SW NW Sec. 8 T11S R23E). This core is located in the field behind the K7 outcrop site (Figure 4).



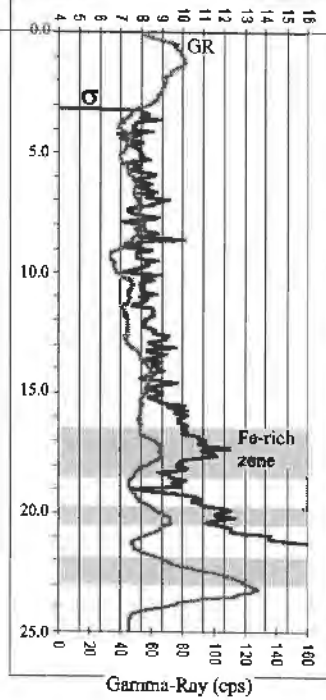
Appendix 1 (cont.) - Lithologic description and K_f values for Core T104 P094 (NE SW NW Sec. 8 T11S R23E). This core is located in the field behind the K7 outcrop site (Figure 4).

T132 P014

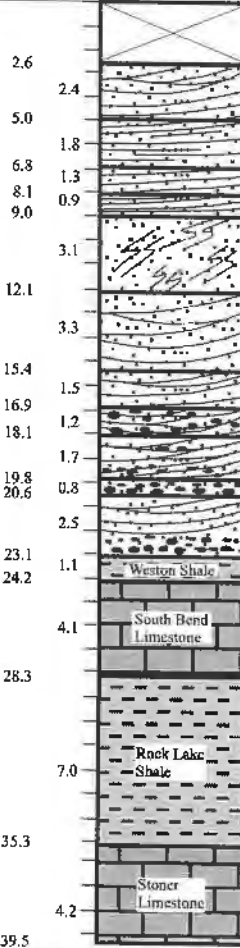
Permeability (md)



Conductivity (mS/m)

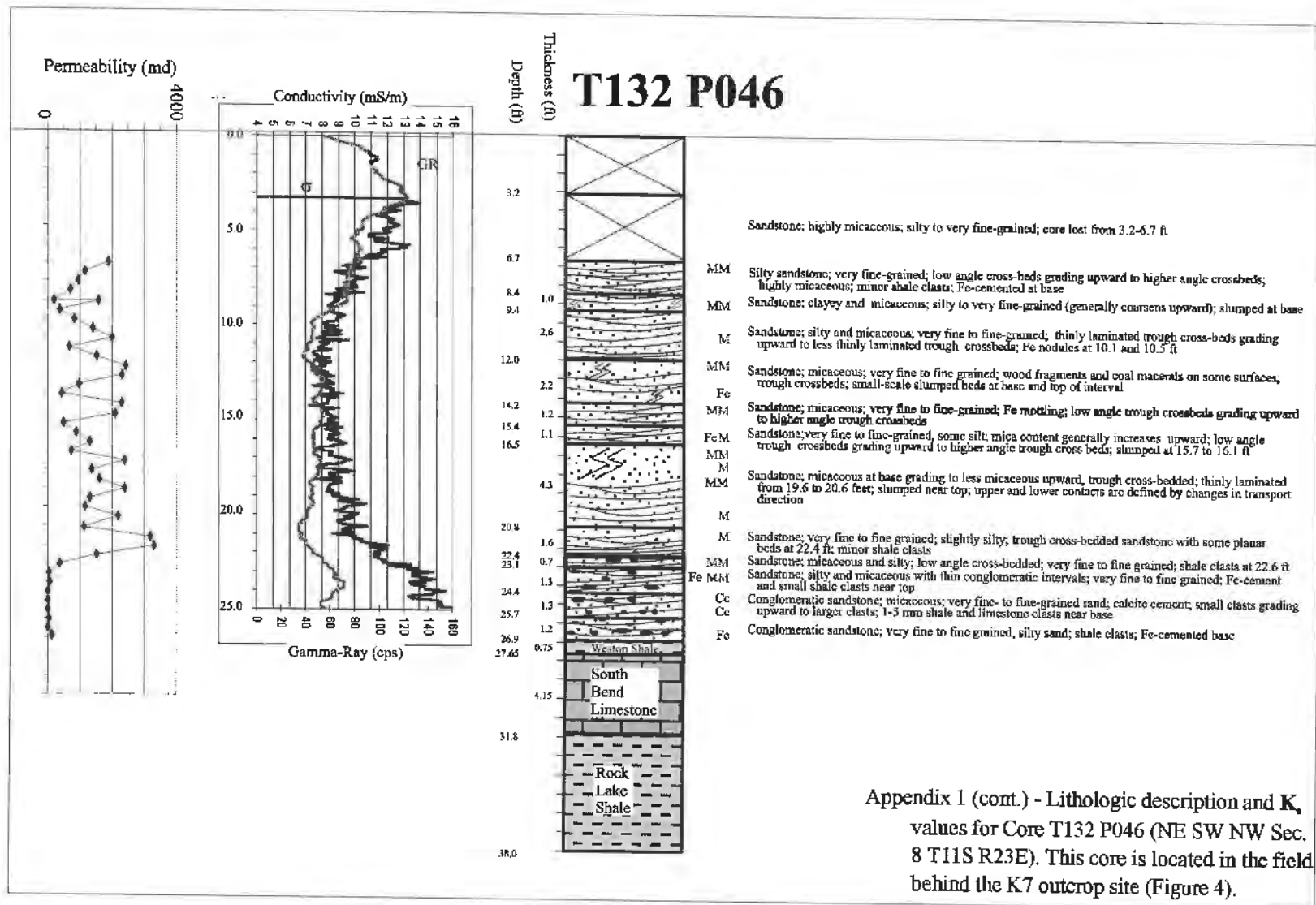


Depth (ft)



- MM Sandstone; trough cross-bedded; Fe cement in some portions
- M
- MM Sandstone; highly micaceous; low angle cross-bedded; poorly indurated near center of zone
- M Sandstone; low angle cross-bedded
- MM Sandstone; highly micaceous; low angle cross-bedded; Fe-cemented at upper contact
- Sandstone; highly convoluted trough cross-bedded
- M
- M Sandstone; trough cross-bedded; coal macerals and mica on cross-bed surfaces
- M
- MM Sandstone; highly micaceous; trough cross-bedded
- M
- Fe MM Conglomeratic sandstone; micaceous; trough cross-bedded; cemented with hydrous Fe-oxide; shale clasts increase in size and number upward
- FeM
- MMM Sandstone; highly micaceous; trough cross-bedded calcite cemented at base; with minor shale clasts near top
- Cc
- Fe Conglomeratic sandstone; clasts decreasing in size upward
- M
- Cc Sandstone; trough cross-bedded; conglomeratic at base; calcite cement; Fe-cemented from 21.0' to 22.1'

Appendix 1 (cont.) - Lithologic description and K_v values for Core T132 P014 (NE SW NW Sec. 8 T11S R23E). This core is located in the field behind the K7 outcrop site (Figure 4).



Appendix I (cont.) - Lithologic description and K_v values for Core T132 P046 (NE SW NW Sec. 8 T11S R23E). This core is located in the field behind the K7 outcrop site (Figure 4).

Appendix 2 - Minipermeameter data and Ka values from analyses of cores from the field behind the fluvial outcrop site

Minipermeameter Data from core T076 P014											
Core	type	depth (ft)	Atm. P (psi)	Upstream P (psi)	Flow Rate (CC/min)	Temp. (deg. F)	Geometric Factor	Tip Radius (inch.)		Ka (md)	Comments
								Inter. R	Exter. R		
T076 P014	H	4.00	13.99	19.80	859.38	87.8	5.1	0.062	0.125	701.0	
T076 P014	H	4.50	13.99	15.82	879.40	88.6	5.1	0.062	0.125	2580.5	suspect measurement
T076 P014	H	5.00	13.99	15.87	888.18	88.8	5.1	0.062	0.125	2534.6	
T076 P014	H	5.50	13.99	15.96	896.48	88.9	5.1	0.062	0.125	2440.1	
T076 P014	H	6.00	13.99	17.48	926.27	89.0	5.1	0.062	0.125	1350.5	
T076 P014	H	6.50	13.99	17.66	929.20	89.2	5.1	0.062	0.125	1279.8	
T076 P014	H	7.00	13.99	16.93	936.04	89.4	5.1	0.062	0.125	1648.4	
T076 P014	H	7.45	13.99	26.04	906.25	89.3	5.1	0.062	0.125	301.0	
T076 P014	H	7.50	13.99	17.32	955.57	89.6	5.1	0.062	0.125	1467.1	
T076 P014	H	8.00	13.99	16.60	957.52	89.9	5.1	0.062	0.125	1919.7	Fe mottled
T076 P014	H	8.50	13.99	18.64	974.12	90.1	5.1	0.062	0.125	1028.4	Fe mottled
T076 P014	H	9.00	13.99	18.36	974.12	90.3	5.1	0.062	0.125	1104.1	Fe mottled
T076 P014	H	9.50	13.99	18.75	979.98	90.7	5.1	0.062	0.125	1007.5	Fe mottled
T076 P014	H	10.00	13.99	21.50	993.65	91.1	5.1	0.062	0.125	597.7	Fe cemented
T076 P014	H	10.50	13.99	19.07	1000.49	91.4	5.1	0.062	0.125	955.1	Fe cemented
T076 P014	H	11.00	13.99	17.14	1022.46	91.1	5.1	0.062	0.125	1671.3	Fe cemented
T076 P014	H	11.50	13.99	18.25	1026.86	91.0	5.1	0.062	0.125	1198.1	Fe mottled
T076 P014	H	12.00	13.99	22.24	1038.57	90.9	5.1	0.062	0.125	556.7	Fe cemented
T076 P014	H	12.50	13.99	34.57	385.99	91.2	5.1	0.062	0.125	61.9	Highly Fe cemented
T076 P014	H	13.00	13.99	18.43	1060.06	90.8	5.1	0.062	0.125	1179.1	Fe cemented conglomerate
T076 P014	H	14.50	13.99	39.04	2.92	91.1	5.1	0.062	0.125	0.4	Cc cemented conglomerate
T076 P014	H	15.00	13.99	39.06	2.63	91.2	5.1	0.062	0.125	0.3	Cc cemented conglomerate
T076 P014	H	15.50	13.99	38.21	5.57	91.2	5.1	0.062	0.125	0.7	Cc cemented conglomerate
T076 P014	H	15.90	13.99	38.49	4.25	91.2	5.1	0.062	0.125	0.5	Cc cemented sandstone

Appendix 2 (cont.)

Minipermeameter Data from core T076 P046											
Core	type	depth (ft)	Atm. P (psi)	Upstream P (psi)	Flow Rate (CC/min)	Temp. (deg. F)	Geometric Factor	Tip Radius (inch.)		Ka (md)	Comments
								Inter. R	Exter. R		
T076 P046	H	0.80	14.04	18.82	961.43	80.6	5.1	0.062	0.125	977.5	
T076 P046	H	1.00	14.04	17.04	973.63	81.4	5.1	0.062	0.125	1668.3	
T076 P046	H	1.50	14.04	16.80	981.45	82.0	5.1	0.062	0.125	1845.3	
T076 P046	H	2.00	14.04	16.20	994.14	82.3	5.1	0.062	0.125	2433.9	
T076 P046	H	2.50	14.04	21.41	1000.98	82.4	5.1	0.062	0.125	612.6	Fe mottled
T076 P046	H	3.00	14.04	21.45	1001.95	83.1	5.1	0.062	0.125	609.6	micaceous
T076 P046	H	3.50	14.04	19.06	1010.25	83.9	5.1	0.062	0.125	973.6	micaceous
T076 P046	H	4.00	14.04	19.34	1017.09	84.3	5.1	0.062	0.125	920.5	micaceous
T076 P046	H	4.50	14.04	18.77	1026.86	84.9	5.1	0.062	0.125	1057.5	micaceous; Fe mottled
T076 P046	H	5.00	14.04	16.37	1035.16	85.5	5.1	0.062	0.125	2337.1	micaceous
T076 P046	H	6.00	14.04	16.64	1049.32	85.9	5.1	0.062	0.125	2106.0	micaceous
T076 P046	H	6.50	14.04	19.78	1056.64	86.4	5.1	0.062	0.125	872.0	
T076 P046	H	7.00	14.04	16.43	1066.90	87.0	5.1	0.062	0.125	2343.4	
T076 P046	H	8.00	14.04	24.50	1080.57	87.2	5.1	0.062	0.125	429.2	
T076 P046	H	8.50	14.04	16.74	1090.82	87.1	5.1	0.062	0.125	2103.8	Fe mottled
T076 P046	H	9.00	14.04	16.83	939.94	87.2	5.1	0.062	0.125	1744.0	micaceous
T076 P046	H	9.50	14.04	19.39	975.10	87.5	5.1	0.062	0.125	873.8	
T076 P046	H	10.00	14.04	32.56	341.31	88.2	5.1	0.062	0.125	63.4	mm-scale lamina
T076 P046	H	10.50	14.04	24.48	955.57	87.9	5.1	0.062	0.125	380.7	micaceous
T076 P046	H	11.00	14.04	18.73	988.28	88.2	5.1	0.062	0.125	1030.6	
T076 P046	H	11.50	14.04	18.43	1010.74	88.4	5.1	0.062	0.125	1134.5	
T076 P046	H	12.00	14.04	21.89	1021.97	88.6	5.1	0.062	0.125	580.5	
T076 P046	H	12.50	14.04	17.03	1041.02	88.9	5.1	0.062	0.125	1794.7	
T076 P046	H	13.00	14.04	18.53	1081.06	88.7	5.1	0.062	0.125	1183.5	
T076 P046	H	13.50	14.01	17.63	876.47	88.7	5.1	0.062	0.125	1227.9	Fe cemented
T076 P046	H	14.00	14.01	17.22	881.84	88.9	5.1	0.062	0.125	1408.5	Fe cemented
T076 P046	H	14.50	14.01	16.60	886.23	88.7	5.1	0.062	0.125	1791.6	mm-scale lamina
T076 P046	H	15.00	14.01	19.35	893.56	88.6	5.1	0.062	0.125	804.2	mm-scale lamina
T076 P046	H	15.50	14.01	15.81	898.93	88.7	5.1	0.062	0.125	2690.6	
T076 P046	H	16.00	14.06	16.08	1189.45	83.4	5.1	0.062	0.125	3134.9	
T076 P046	H	16.50	14.06	16.05	924.81	84.2	5.1	0.062	0.125	2469.7	
T076 P046	H	17.00	14.04	15.91	1370.61	78.4	5.1	0.062	0.125	3916.2	
T076 P046	H	17.50	14.04	16.14	1390.63	79.8	5.1	0.062	0.125	3508.5	

Minipermeameter Data from core T076 P046

Core	type	depth (ft)	Atm. P (psi)	Upstream P (psi)	Flow Rate (CC/min)	Temp. (deg. F)	Geometric Factor	Tip Radius (inch.)		Ka (md)	Comments
								Inter. R	Exter. R		
T076 P046	H	18.00	14.04	17.51	1419.43	81.4	5.1	0.062	0.125	2075.7	
T076 P046	H	18.50	14.04	16.71	1441.90	82.2	5.1	0.062	0.125	2805.5	
T076 P046	H	19.00	14.04	16.10	1466.31	83.5	5.1	0.062	0.125	3773.1	
T076 P046	H	19.50	14.04	22.34	1499.02	83.8	5.1	0.062	0.125	794.3	highly micaceous
T076 P046	H	20.00	14.04	34.42	1433.59	84.5	5.1	0.062	0.125	232.2	highly Fe cemented
T076 P046	H	20.50	14.04	39.27	759.77	85.2	5.1	0.062	0.125	90.4	highly Fe cemented
T076 P046	H	21.00	14.04	43.41	6.07	86.1	5.1	0.062	0.125	0.6	Fe and calcite cemented
T076 P046	H	21.50	14.04	44.13	3.06	86.9	5.1	0.062	0.125	0.3	Fe and calcite cemented
T076 P046	H	22.00	14.04	36.90	1237.31	87.0	5.1	0.062	0.125	170.1	highly Fe cemented
T076 P046	H	22.50	14.04	16.08	1570.80	87.9	5.1	0.062	0.125	4097.7	suspect measurement
T076 P046	H	23.00	14.04	46.99	2.33	86.1	5.1	0.062	0.125	0.2	calcite cemented conglomerate
T076 P046	H	23.50	14.04	47.08	2.86	87.0	5.1	0.062	0.125	0.2	calcite cemented conglomerate
T076 P046	H	24.00	14.04	46.81	4.40	87.6	5.1	0.062	0.125	0.4	calcite cemented conglomerate

Appendix 2 (cont.)

Minipermeameter Data from core T104 P014											
Core	type	depth (ft)	Atm. P (psi)	Upstream P (psi)	Flow Rate (CC/min)	Temp. (deg. F)	Geometric Factor	Tip Radius (inch.)		Ka (md)	Comments
								Inter. R	Exter. R		
T104 P014	H	2.50	13.98	17.20	1404.00	75.0	5.1	0.062	0.125	2247.0	
T104 P014	H	2.75	13.98	16.72	1456.00	75.8	5.1	0.062	0.125	2761.0	
T104 P014	H	3.00	13.98	16.58	1504.00	76.5	5.1	0.062	0.125	3043.0	
T104 P014	H	3.25	13.98	18.74	1479.00	77.3	5.1	0.062	0.125	1526.0	
T104 P014	H	3.50	13.98	17.38	1501.00	78.0	5.1	0.062	0.125	2262.0	
T104 P014	H	3.75	13.98	22.00	1518.00	78.8	5.1	0.062	0.125	842.0	
T104 P014	H	4.00	13.98	30.26	1539.00	79.5	5.1	0.062	0.125	340.0	
T104 P014	H	4.25	13.98	24.55	1537.00	80.3	5.1	0.062	0.125	606.0	
T104 P014	H	4.50	13.98	21.69	1541.00	81.0	5.1	0.062	0.125	897.0	
T104 P014	H	4.75	13.98	19.68	1549.00	81.8	5.1	0.062	0.125	1297.0	
T104 P014	H	5.00	13.98	21.15	1557.00	82.5	5.1	0.062	0.125	988.0	
T104 P014	H	5.25	13.98	22.95	1574.00	83.3	5.1	0.062	0.125	765.0	
T104 P014	H	5.50	13.98	17.57	1577.00	84.0	5.1	0.062	0.125	2231.0	
T104 P014	H	5.75	13.98	23.69	1594.00	84.8	5.1	0.062	0.125	700.0	
T104 P014	H	6.00	13.98	22.69	1606.00	85.5	5.1	0.062	0.125	806.3	
T104 P014	H	6.25	13.98	34.14	1622.00	86.3	5.1	0.062	0.125	268.0	
T104 P014	H	6.50	14.12	34.56	794.43	79.5	5.1	0.062	0.125	127.6	
T104 P014	H	6.75	14.12	16.76	1443.85	83.0	5.1	0.062	0.125	2836.5	
T104 P014	H	7.00	14.12	17.73	1457.52	83.7	5.1	0.062	0.125	2033.4	
T104 P014	H	7.25	14.12	17.35	1468.26	85.2	5.1	0.062	0.125	2317.2	
T104 P014	H	7.50	14.12	24.51	1484.86	85.5	5.1	0.062	0.125	592.2	slumped bedding
T104 P014	H	7.75	14.12	20.47	1490.23	86.2	5.1	0.062	0.125	1086.4	Fe mottling
T104 P014	H	8.00	14.12	27.80	1504.88	86.4	5.1	0.062	0.125	420.4	
T104 P014	H	8.25	14.12	26.07	1521.97	87.4	5.1	0.062	0.125	507.3	Slumped; Fe mottling
T104 P014	H	8.50	14.12	22.63	1544.43	86.7	5.1	0.062	0.125	790.7	
T104 P014	H	9.00	14.12	17.46	1565.43	87.6	5.1	0.062	0.125	2382.0	
T104 P014	H	9.25	14.12	16.11	690.92	88.4	5.1	0.062	0.125	1839.3	
T104 P014	H	9.50	14.12	16.65	695.80	88.7	5.1	0.062	0.125	1433.2	
T104 P014	H	9.75	14.12	24.51	703.13	88.4	5.1	0.062	0.125	280.6	
T104 P014	H	10.00	14.12	17.30	707.03	88.8	5.1	0.062	0.125	1135.6	
T104 P014	H	10.25	14.12	16.37	717.77	87.6	5.1	0.062	0.125	1678.2	
T104 P014	H	10.50	14.12	16.70	722.66	88.3	5.1	0.062	0.125	1457.9	
T104 P014	H	10.65	14.12	18.99	727.54	89.1	5.1	0.062	0.125	722.5	

Minipermeameter Data from core T104 P014

Core	type	depth (ft)	Atm. P (psi)	Upstream P (psi)	Flow Rate (CC/min)	Temp. (deg. F)	Geometric Factor	Tip Radius (inch.)		Ka (md)	Comments
								Inter. R	Exter. R		
T104 P014	H	10.75	14.12	18.70	733.89	88.9	5.1	0.062	0.125	782.3	
T104 P014	H	11.25	14.12	23.41	744.14	88.3	5.1	0.062	0.125	341.8	
T104 P014	H	11.50	14.12	19.18	743.65	88.5	5.1	0.062	0.125	707.7	Fe cement
T104 P014	H	11.75	14.12	17.85	748.05	88.6	5.1	0.062	0.125	1006.6	Fe cement
T104 P014	H	12.00	14.12	20.01	753.91	89.4	5.1	0.062	0.125	601.4	Fe cement
T104 P014	H	12.25	14.12	16.91	757.81	89.6	5.1	0.062	0.125	1405.7	Fe cement
T104 P014	H	12.50	14.12	21.78	1646.48	90.5	5.1	0.062	0.125	960.1	Fe cement - less than above
T104 P014	H	12.75	14.09	17.20	1601.56	81.1	5.1	0.062	0.125	2629.6	Fe cement - less than above
T104 P014	H	13.00	14.09	23.62	702.15	82.5	5.1	0.062	0.125	312.4	High amt. of Fe cem.
T104 P014	H	13.35	14.09	31.84	703.13	83.9	5.1	0.062	0.125	138.0	High amt. of Fe cem.
T104 P014	H	13.50	14.09	36.07	704.10	84.5	5.1	0.062	0.125	102.2	High amt. of Fe cem.
T104 P014	H	13.75	14.09	35.78	706.06	85.0	5.1	0.062	0.125	104.5	High amt. of Fe cem.
T104 P014	H	14.00	14.09	32.28	700.20	85.4	5.1	0.062	0.125	132.9	High amt. of Fe cem.
T104 P014	H	14.25	14.09	35.36	710.45	86.0	5.1	0.062	0.125	108.1	Fe and calcite cement
T104 P014	H	14.50	14.09	49.99	2.08	87.7	5.1	0.062	0.125	0.1	
T104 P014	H	14.75	14.09	49.99	4.69	88.9	5.1	0.062	0.125	0.3	
T104 P014	H	15.00	14.09	49.99	919.92	88.6	5.1	0.062	0.125	64.1	
T104 P014	H	15.25	14.09	34.50	4.07	87.5	5.1	0.062	0.125	0.7	silty sandstone
T104 P014	H	15.40	14.09	35.27	3.48	88.8	5.1	0.062	0.125	0.5	
T104 P014	H	15.75	14.09	17.43	1257.32	89.2	5.1	0.062	0.125	1910.5	High amt. of Fe cem. calcite cement
T104 P014	H	16.25	14.09	32.62	767.58	89.5	5.1	0.062	0.125	142.1	High amt. of Fe cem.
T104 P014	H	16.50	14.09	33.00	782.23	89.8	5.1	0.062	0.125	140.8	High amt. of Fe cem.
T104 P014	H	17.00	14.09	32.67	903.32	90.2	5.1	0.062	0.125	166.6	High amt. of Fe cem.
T104 P014	H	17.25	14.09	20.92	1327.15	90.2	5.1	0.062	0.125	888.5	High amt. of Fe cem.
T104 P014	H	17.50	14.09	26.65	1331.06	89.8	5.1	0.062	0.125	416.8	High amt. of Fe cem.
T104 P014	H	17.75	14.09	33.52	1029.79	90.2	5.1	0.062	0.125	178.3	High amt. of Fe cem.
T104 P014	H	18.00	14.09	20.25	1351.07	90.4	5.1	0.062	0.125	1022.7	Fe mottling
T104 P014	H	18.25	14.09	21.36	1363.77	90.8	5.1	0.062	0.125	847.3	Fe mottling
T104 P014	H	18.50	14.09	23.30	1381.84	91.2	5.1	0.062	0.125	642.6	Fe mottling
T104 P014	H	18.75	14.09	26.49	1387.70	91.4	5.1	0.062	0.125	441.9	Fe mottling
T104 P014	H	19.00	14.09	18.68	1401.86	90.5	5.1	0.062	0.125	1493.7	Fe mottling
T104 P014	H	19.25	14.09	19.12	1409.18	90.8	5.1	0.062	0.125	1352.2	Fe mottling
T104 P014	H	19.50	14.09	21.03	1416.50	91.0	5.1	0.062	0.125	930.5	Fe mottling
T104 P014	H	19.75	14.09	22.14	1423.34	91.2	5.1	0.062	0.125	781.4	Fe mottling
T104 P014	H	19.90	14.09	20.34	1451.66	91.0	5.1	0.062	0.125	1081.2	Fe mottling
T104 P014	H	20.00	14.09	30.70	1432.13	91.4	5.1	0.062	0.125	308.4	Fe mottling

Appendix 2 (cont.)

Minipermeameter Data from core T104 P030											
Core	type	depth (ft)	Atm. P (psi)	Upstream P (psi)	Flow Rate (CC/min)	Temp. (deg. F)	Geometric Factor	Tip Radius (inch.)		Ka (md)	Comments
								Inter. R	Exter. R		
T104 P030	H	8.50	14.04	17.14	1401.37	84.8	5.1	0.062	0.125	2320.1	
T104 P030	H	9.00	14.04	18.75	1427.25	85.3	5.1	0.062	0.125	1478.6	
T104 P030	H	9.50	14.04	17.57	1437.99	85.5	5.1	0.062	0.125	2064.5	
T104 P030	H	10.00	14.04	20.11	1453.13	86.1	5.1	0.062	0.125	1123.0	
T104 P030	H	10.50	14.04	17.31	1469.73	86.4	5.1	0.062	0.125	2294.4	
T104 P030	H	11.00	14.04	18.69	1489.26	86.7	5.1	0.062	0.125	1566.5	
T104 P030	H	11.50	14.04	19.41	1493.65	87.2	5.1	0.062	0.125	1331.3	
T104 P030	H	12.00	14.04	30.62	1507.81	87.2	5.1	0.062	0.125	326.2	
T104 P030	H	12.50	14.04	23.63	1515.14	87.4	5.1	0.062	0.125	671.3	
T104 P030	H	13.00	14.04	16.42	1562.01	89.1	5.1	0.062	0.125	3451.3	
T104 P030	H	13.50	14.04	21.66	1583.50	88.7	5.1	0.062	0.125	932.9	
T104 P030	H	14.00	14.04	19.19	1598.15	88.4	5.1	0.062	0.125	1495.4	
T104 P030	H	14.50	14.04	18.12	1608.89	88.6	5.1	0.062	0.125	1965.7	
T104 P030	H	15.00	14.04	17.16	1613.77	88.8	5.1	0.062	0.125	2651.0	
T104 P030	H	15.50	14.04	19.18	1625.00	89.3	5.1	0.062	0.125	1525.0	
T104 P030	H	16.00	14.04	17.43	1637.70	89.2	5.1	0.062	0.125	2456.5	
T104 P030	H	16.50	14.04	21.66	1655.27	89.5	5.1	0.062	0.125	975.3	
T104 P030	H	17.00	14.04	18.02	1666.50	89.6	5.1	0.062	0.125	2092.9	
T104 P030	H	17.50	14.04	28.33	1680.66	89.7	5.1	0.062	0.125	444.6	
T104 P030	H	18.00	14.04	18.86	1686.04	89.8	5.1	0.062	0.125	1702.9	Fe cement
T104 P030	H	18.50	14.03	21.56	1028.81	79.5	5.1	0.062	0.125	613.6	
T104 P030	H	19.00	14.03	18.52	1147.95	80.6	5.1	0.062	0.125	1255.4	Fe cement
T104 P030	H	19.50	14.03	16.81	1164.55	81.4	5.1	0.062	0.125	2170.0	
T104 P030	H	20.00	14.03	17.33	1176.27	82.0	5.1	0.062	0.125	1813.4	
T104 P030	H	20.50	14.03	16.13	1279.79	89.2	5.1	0.062	0.125	3238.3	
T104 P030	H	21.00	14.03	17.74	1320.31	89.7	5.1	0.062	0.125	1794.6	Fe cement
T104 P030	H	21.50	14.01	17.79	1380.86	89.3	5.1	0.062	0.125	1844.2	Cgl; Fe cemented
T104 P030	H	22.00	14.01	36.83	703.61	89.6	5.1	0.062	0.125	97.2	Fe cement
T104 P030	H	22.50	14.01	22.03	1395.02	88.7	5.1	0.062	0.125	772.9	
T104 P030	H	23.00	14.01	24.28	1402.83	88.7	5.1	0.062	0.125	571.6	
T104 P030	H	23.50	14.01	21.29	1417.97	89.2	5.1	0.062	0.125	884.4	
T104 P030	H	24.00	14.01	24.73	1429.69	89.3	5.1	0.062	0.125	551.5	
T104 P030	H	24.50	14.01	29.80	1448.73	89.0	5.1	0.062	0.125	335.6	

Appendix 2 (cont.)

Minipermeameter Data from core T104 P046											
Core	type	depth (ft)	Atm. P (psi)	Upstream P (psi)	Flow Rate (CC/min)	Temp. (deg. F)	Geometric Factor	Tip Radius (inch.)		Ka (md)	Comments
								Inter. R	Exter. R		
T104 P046	H	3.50	14.01	30.23	1560.06	78.9	5.1	0.062	0.125	347.7	
T104 P046	H	4.00	14.01	25.42	1572.27	80.5	5.1	0.062	0.125	559.2	
T104 P046	H	4.50	14.01	21.24	1600.59	83.1	5.1	0.062	0.125	1005.1	
T104 P046	H	5.00	14.01	19.95	1605.96	84.6	5.1	0.062	0.125	1275.7	
T104 P046	H	5.50	14.01	20.95	1624.51	86.1	5.1	0.062	0.125	1072.8	
T104 P046	H	6.00	14.00	24.01	1620.12	83.3	5.1	0.062	0.125	681.2	
T104 P046	H	6.50	14.00	22.88	1640.63	83.6	5.1	0.062	0.125	802.1	
T104 P046	H	7.00	14.00	22.84	1648.44	86.3	5.1	0.062	0.125	810.5	
T104 P046	H	7.50	14.00	20.35	1659.67	87.0	5.1	0.062	0.125	1218.7	
T104 P046	H	8.00	14.00	20.61	1664.55	87.8	5.1	0.062	0.125	1166.4	
T104 P046	H	8.50	14.00	22.94	1676.27	88.6	5.1	0.062	0.125	813.4	
T104 P046	H	9.00	14.00	17.48	1689.45	88.8	5.1	0.062	0.125	2470.7	
T104 P046	H	9.50	14.00	37.33	1704.59	88.7	5.1	0.062	0.125	228.0	
T104 P046	H	10.00	14.00	49.99	910.65	88.8	5.1	0.062	0.125	63.3	Fe-rich
T104 P046	H	10.50	14.00	17.25	1103.03	86.9	5.1	0.062	0.125	1740.5	
T104 P046	H	11.00	14.00	17.32	1124.51	88.3	5.1	0.062	0.125	1731.7	
T104 P046	H	11.50	14.00	19.58	1144.04	88.7	5.1	0.062	0.125	978.1	Fe stains
T104 P046	H	12.00	14.00	16.20	1173.83	89.3	5.1	0.062	0.125	2833.7	
T104 P046	H	12.50	14.00	18.47	1190.43	89.5	5.1	0.062	0.125	1314.6	
T104 P046	H	13.00	14.00	25.53	1136.72	89.6	5.1	0.062	0.125	399.8	Fe stains
T104 P046	H	13.50	14.00	16.80	1219.24	89.6	5.1	0.062	0.125	2268.8	Fe stains
T104 P046	H	14.00	14.00	22.36	1227.54	90.1	5.1	0.062	0.125	646.8	slumped bedding
T104 P046	H	14.50	14.00	21.84	1237.79	90.3	5.1	0.062	0.125	706.1	Fe stains
T104 P046	H	15.00	14.00	16.41	1256.84	89.2	5.1	0.062	0.125	2753.3	
T104 P046	H	15.50	14.00	16.70	1278.32	89.4	5.1	0.062	0.125	2472.5	
T104 P046	H	16.00	14.00	19.10	1288.57	89.1	5.1	0.062	0.125	1221.9	
T104 P046	H	16.50	14.00	23.45	1303.71	89.6	5.1	0.062	0.125	590.3	
T104 P046	H	17.00	14.00	24.30	1310.55	89.5	5.1	0.062	0.125	532.0	
T104 P046	H	17.50	14.00	18.38	1320.80	89.6	5.1	0.062	0.125	1490.9	
T104 P046	H	18.00	14.00	20.63	1330.57	89.6	5.1	0.062	0.125	928.6	
T104 P046	H	18.50	14.00	21.50	1340.82	89.5	5.1	0.062	0.125	807.3	
T104 P046	H	19.00	14.00	29.25	1351.56	90.0	5.1	0.062	0.125	328.4	
T104 P046	H	19.50	14.00	19.15	1373.05	90.2	5.1	0.062	0.125	1286.1	

Minipermeameter Data from core T104 P046

Core	type	depth (ft)	Atm. P (psi)	Upstream P (psi)	Flow Rate (CC/min)	Temp. (deg. F)	Geometric Factor	Tip Radius (inch.)		Ka (md)	Comments
								Inter. R	Exter. R		
T104 P046	H	20.00	14.00	26.25	1387.70	90.0	5.1	0.062	0.125	451.2	
T104 P046	H	20.50	14.00	17.24	1399.41	90.6	5.1	0.062	0.125	2219.0	
T104 P046	H	21.00	14.00	18.47	1416.02	90.5	5.1	0.062	0.125	1564.0	
T104 P046	H	21.50	14.00	16.81	1429.69	90.2	5.1	0.062	0.125	2648.0	
T104 P046	H	22.00	14.00	18.71	1439.45	90.3	5.1	0.062	0.125	1496.2	
T104 P046	H	22.50	14.00	29.96	1458.50	90.6	5.1	0.062	0.125	333.2	
T104 P046	H	23.00	14.00	21.67	1474.12	91.0	5.1	0.062	0.125	863.9	Fe mottling
T104 P046	H	23.50	14.00	34.12	1487.79	91.1	5.1	0.062	0.125	246.3	Fe cement
T104 P046	H	24.00	14.00	46.83	4.98	91.6	5.1	0.062	0.125	0.4	Fe; calcite cement
T104 P046	H	24.50	14.00	47.19	3.89	91.8	5.1	0.062	0.125	0.3	Fe; calcite cement
T104 P046	H	25.00	14.00	46.56	8.24	92.1	5.1	0.062	0.125	0.7	Fe; calcite cement
T104 P046	H	25.50	14.00	46.80	6.59	92.3	5.1	0.062	0.125	0.5	Fe; calcite cement
T104 P046	H	26.00	14.00	47.08	8.79	92.6	5.1	0.062	0.125	0.7	calcite cement; Fe
T104 P046	H	26.50	14.00	47.38	5.42	92.6	5.1	0.062	0.125	0.4	calcite cement
T104 P046	H	27.00	14.00	47.66	4.42	92.4	5.1	0.062	0.125	0.3	calcite cement

Appendix 2 (cont.)

Minipermeameter Data from core T104 P062											
Core	type	depth (ft)	Atm. P (psi)	Upstream P (psi)	Flow Rate (CC/min)	Temp. (deg. F)	Geometric Factor	Tip Radius (inch.)		Ka (md)	Comments
								Inter. R	Exter. R		
T104 P062	H	5.00	14.06	23.66	715.82	78.1	5.1	0.062	0.125	316.0	
T104 P062	H	5.50	14.06	22.36	895.51	79.8	5.1	0.062	0.125	473.4	
T104 P062	H	6.00	14.06	23.22	832.52	80.7	5.1	0.062	0.125	390.0	
T104 P062	H	6.50	14.06	19.09	1064.94	83.4	5.1	0.062	0.125	1021.8	
T104 P062	H	7.00	14.06	21.70	1067.87	84.8	5.1	0.062	0.125	625.3	
T104 P062	H	7.50	14.06	22.73	1021.48	84.9	5.1	0.062	0.125	512.7	
T104 P062	H	8.00	14.06	23.12	1019.53	84.9	5.1	0.062	0.125	484.5	
T104 P062	H	8.50	14.06	20.59	1106.93	85.1	5.1	0.062	0.125	782.8	
T104 P062	H	9.00	14.06	21.75	1115.23	85.3	5.1	0.062	0.125	648.1	
T104 P062	H	9.50	14.06	23.15	1112.79	85.3	5.1	0.062	0.125	527.1	
T104 P062	H	10.00	14.06	19.71	1133.30	86.4	5.1	0.062	0.125	950.4	
T104 P062	H	10.50	14.06	16.44	1145.51	86.6	5.1	0.062	0.125	2525.7	
T104 P062	H	11.00	14.06	17.32	1160.65	87.5	5.1	0.062	0.125	1817.0	
T104 P062	H	11.50	14.06	16.35	1324.71	87.9	5.1	0.062	0.125	3056.4	
T104 P062	H	12.00	14.06	18.86	1338.87	87.6	5.1	0.062	0.125	1357.5	
T104 P062	H	12.50	14.06	18.20	1350.10	87.7	5.1	0.062	0.125	1619.4	
T104 P062	H	13.00	14.06	17.08	1359.86	87.9	5.1	0.062	0.125	2319.5	
T104 P062	H	13.50	14.06	25.65	1373.05	88.4	5.1	0.062	0.125	478.1	
T104 P062	H	14.00	14.06	20.28	1383.30	88.2	5.1	0.062	0.125	1038.4	
T104 P062	H	14.50	14.06	20.40	1388.18	86.9	5.1	0.062	0.125	1018.1	
T104 P062	H	15.00	14.06	17.25	1398.93	86.7	5.1	0.062	0.125	2245.2	
T104 P062	H	15.50	14.06	16.49	913.09	86.7	5.1	0.062	0.125	1969.7	
T104 P062	H	16.00	14.06	25.13	918.95	86.5	5.1	0.062	0.125	339.0	
T104 P062	H	16.50	14.06	33.67	809.57	86.7	5.1	0.062	0.125	138.5	
T104 P062	H	17.00	14.06	19.18	926.27	86.5	5.1	0.062	0.125	872.3	
T104 P062	H	17.50	14.06	17.33	927.73	87.2	5.1	0.062	0.125	1446.3	
T104 P062	H	18.00	14.06	16.27	933.11	87.7	5.1	0.062	0.125	2229.5	
T104 P062	H	18.50	14.06	16.96	937.50	88.0	5.1	0.062	0.125	1673.1	
T104 P062	H	19.00	14.06	16.91	942.87	87.4	5.1	0.062	0.125	1714.1	
T104 P062	H	19.50	14.06	17.80	948.73	86.9	5.1	0.062	0.125	1276.4	
T104 P062	H	20.00	14.06	15.64	955.57	87.0	5.1	0.062	0.125	3271.5	
T104 P062	H	20.50	14.06	16.06	959.96	87.0	5.1	0.062	0.125	2548.5	
T104 P062	H	21.00	14.04	17.32	838.87	83.2	5.1	0.062	0.125	1303.3	Fe mottled

Minipermeameter Data from core T104 P062

Core	type	depth (ft)	Atm. P (psi)	Upstream P (psi)	Flow Rate (CC/min)	Temp. (deg. F)	Geometric Factor	Tip Radius (inch.)		Ka (md)	Comments
								Inter. R	Exter. R		
T104 P062	H	21.50	14.04	16.44	846.68	83.7	5.1	0.062	0.125	1848.1	Fe mottled
T104 P062	H	22.00	14.04	17.71	852.05	83.9	5.1	0.062	0.125	1168.7	Fe mottled
T104 P062	H	22.50	14.04	17.22	858.40	84.6	5.1	0.062	0.125	1379.2	Fe cemented
T104 P062	H	23.00	14.04	24.37	867.68	84.8	5.1	0.062	0.125	350.1	Fe cemented
T104 P062	H	23.50	14.04	32.07	862.31	85.3	5.1	0.062	0.125	166.0	Fe cemented conglomerate
T104 P062	H	24.00	14.04	45.28	2.84	85.3	5.1	0.062	0.125	0.2	Fe cemented conglomerate
T104 P062	H	24.50	14.04	44.45	4.27	86.2	5.1	0.062	0.125	0.4	Calcite cemented conglomerate
T104 P062	H	25.00	14.04	45.33	2.84	86.6	5.1	0.062	0.125	0.2	Calcite cemented conglomerate
T104 P062	H	25.50	14.04	45.44	3.61	87.0	5.1	0.062	0.125	0.3	Calcite cemented conglomerate
T104 P062	H	26.00	14.04	45.68	2.28	87.2	5.1	0.062	0.125	0.2	Calcite cemented conglomerate
T104 P062	H	26.50	14.04	45.47	3.92	87.3	5.1	0.062	0.125	0.3	Calcite cemented conglomerate
T104 P062	H	27.00	14.04	45.74	2.52	87.4	5.1	0.062	0.125	0.2	Calcite cemented conglomerate
T104 P062	H	27.50	14.04	45.74	2.80	87.6	5.1	0.062	0.125	0.2	Calcite cemented conglomerate

Appendix 2 (cont.)

Minipermeameter Data from core T104 P078											
Core	type	depth (ft)	Atm. P (psi)	Upstream P (psi)	Flow Rate (CC/min)	Temp. (deg. F)	Geometric Factor	Tip Radius (Inch.)		Ka (md)	Comments
								Inter. R	Exter. R		
T104 P078	H	4.00	14.08	23.13	881.35	88.7	5.1	0.062	0.125	418.9	
T104 P078	H	4.50	14.08	22.61	954.10	89.0	5.1	0.062	0.125	488.3	
T104 P078	H	5.00	14.08	25.54	669.43	89.3	5.1	0.062	0.125	236.2	
T104 P078	H	5.50	14.08	24.79	773.93	89.5	5.1	0.062	0.125	297.6	
T104 P078	H	6.00	14.08	19.14	1001.47	89.9	5.1	0.062	0.125	953.5	
T104 P078	H	6.50	14.08	17.99	1010.25	90.1	5.1	0.062	0.125	1288.1	
T104 P078	H	7.00	14.08	18.18	1015.14	90.2	5.1	0.062	0.125	1229.6	
T104 P078	H	7.50	14.08	19.96	1021.48	90.4	5.1	0.062	0.125	817.4	Fe cemented
T104 P078	H	8.00	14.08	16.94	1031.25	90.6	5.1	0.062	0.125	1857.1	
T104 P078	H	8.50	14.08	16.20	1044.43	90.5	5.1	0.062	0.125	2602.6	
T104 P078	H	9.00	14.08	16.11	1045.41	90.7	5.1	0.062	0.125	2722.0	
T104 P078	H	9.50	14.08	16.80	1049.81	91.1	5.1	0.062	0.125	2001.8	
T104 P078	H	10.00	14.08	17.27	1065.92	91.4	5.1	0.062	0.125	1703.8	
T104 P078	H	10.50	14.08	16.44	859.86	91.6	5.1	0.062	0.125	1906.8	Fe mottled
T104 P078	H	11.00	14.08	16.79	872.56	92.1	5.1	0.062	0.125	1672.3	Fe mottled
T104 P078	H	11.50	14.08	16.33	880.37	91.8	5.1	0.062	0.125	2054.7	Fe mottled
T104 P078	H	12.00	14.08	16.33	881.84	91.4	5.1	0.062	0.125	2058.0	Fe mottled
T104 P078	H	12.50	14.08	15.93	883.79	90.7	5.1	0.062	0.125	2543.7	
T104 P078	H	13.00	14.08	17.00	888.67	90.0	5.1	0.062	0.125	1563.7	
T104 P078	H	13.50	14.08	17.69	896.97	90.8	5.1	0.062	0.125	1252.4	
T104 P078	H	14.00	14.08	16.53	899.90	90.5	5.1	0.062	0.125	1920.3	
T104 P078	H	14.50	14.08	15.99	900.88	89.9	5.1	0.062	0.125	2504.8	micaceous
T104 P078	H	15.00	14.08	18.76	909.67	90.1	5.1	0.062	0.125	946.9	micaceous
T104 P078	H	15.50	14.08	17.91	917.48	90.5	5.1	0.062	0.125	1199.2	micaceous
T104 P078	H	16.00	14.08	18.07	915.53	90.6	5.1	0.062	0.125	1143.4	
T104 P078	H	16.50	14.08	18.23	920.90	91.0	5.1	0.062	0.125	1100.8	micaceous
T104 P078	H	17.00	14.08	21.55	933.11	88.6	5.1	0.062	0.125	561.6	micaceous
T104 P078	H	17.50	14.08	17.26	931.64	89.3	5.1	0.062	0.125	1494.9	
T104 P078	H	18.00	14.08	15.64	940.92	89.7	5.1	0.062	0.125	3247.0	
T104 P078	H	18.50	14.08	18.52	947.27	89.4	5.1	0.062	0.125	1047.8	
T104 P078	H	19.00	14.08	17.51	950.20	89.4	5.1	0.062	0.125	1405.2	
T104 P078	H	19.50	14.08	23.77	959.96	89.4	5.1	0.062	0.125	419.3	
T104 P078	H	20.00	14.08	16.74	960.94	89.8	5.1	0.062	0.125	1877.7	

Minipermeameter Data from core T104 P078

Core	type	depth (ft)	Atm. P (psi)	Upstream P (psi)	Flow Rate (CC/min)	Temp. (deg. F)	Geometric Factor	Tip Radius (inch.)		Ka (md)	Comments
								Inter. R	Exter. R		
T104 P078	H	20.50	14.08	16.30	966.31	90.0	5.1	0.062	0.125	2294.5	
T104 P078	H	21.00	14.08	17.60	968.26	90.3	5.1	0.062	0.125	1388.3	Fe cemented
T104 P078	H	21.50	14.08	16.64	976.07	90.4	5.1	0.062	0.125	1986.4	Fe mottled
T104 P078	H	22.00	14.08	17.51	982.91	90.6	5.1	0.062	0.125	1453.9	Fe mottled
T104 P078	H	22.50	14.08	18.48	984.86	90.6	5.1	0.062	0.125	1100.0	Fe mottled
T104 P078	H	23.00	14.04	18.68	1292.97	90.5	5.1	0.062	0.125	1365.2	Fe cemented
T104 P078	H	23.50	14.04	23.55	1375.00	90.7	5.1	0.062	0.125	616.5	Fe cemented
T104 P078	H	24.00	14.04	16.82	1440.43	90.8	5.1	0.062	0.125	2687.4	
T104 P078	H	24.50	14.04	18.34	1465.82	90.5	5.1	0.062	0.125	1688.5	micaceous
T104 P078	H	25.00	14.04	16.32	1483.89	90.6	5.1	0.062	0.125	3431.0	
T104 P078	H	26.00	14.04	47.10	3.20	91.0	5.1	0.062	0.125	0.3	Calcite cement
T104 P078	H	26.50	14.04	47.19	2.97	90.9	5.1	0.062	0.125	0.2	Calcite cement
T104 P078	H	27.00	14.04	16.77	1504.40	90.9	5.1	0.062	0.125	2861.4	highly Fe cemented
T104 P078	H	28.00	14.04	27.31	1597.66	90.2	5.1	0.062	0.125	466.6	highly Fe cemented
T104 P078	H	28.50	14.04	34.95	1596.68	90.2	5.1	0.062	0.125	249.7	highly Fe cemented

Appendix 2 (cont.)

Minipermeameter Data from core T104 P094											
Core	type	depth (ft)	Atm. P (psi)	Upstream P (psi)	Flow Rate (CC/min)	Temp. (deg. F)	Geometric Factor	Tip Radius (inch.)		Ka (md)	Comments
								Inter. R	Exter. R		
T104 P094	H	4.00	13.99	18.51	712.89	80.3	5.1	0.062	0.125	776.5	
T104 P094	H	4.50	13.99	19.20	637.21	81.2	5.1	0.062	0.125	589.0	
T104 P094	H	5.00	13.99	22.83	104.13	81.6	5.1	0.062	0.125	51.2	
T104 P094	H	5.50	13.99	19.76	652.83	81.8	5.1	0.062	0.125	535.7	
T104 P094	H	6.00	13.99	19.02	752.93	82.2	5.1	0.062	0.125	725.4	
T104 P094	H	6.50	13.99	18.91	782.72	82.7	5.1	0.062	0.125	773.6	
T104 P094	H	7.00	13.99	17.53	923.34	83.5	5.1	0.062	0.125	1324.0	
T104 P094	H	7.50	13.99	19.58	779.30	84.2	5.1	0.062	0.125	664.4	
T104 P094	H	8.00	13.99	18.15	932.13	84.7	5.1	0.062	0.125	1115.0	
T104 P094	H	8.50	13.99	15.82	974.12	85.8	5.1	0.062	0.125	2856.8	
T104 P094	H	9.00	13.99	16.17	987.31	87.0	5.1	0.062	0.125	2398.5	
T104 P094	H	9.50	13.99	15.88	1105.96	88.2	5.1	0.062	0.125	3134.0	
T104 P094	H	10.00	13.99	16.53	1120.12	88.6	5.1	0.062	0.125	2315.4	
T104 P094	H	10.50	13.99	19.60	906.74	88.6	5.1	0.062	0.125	769.9	
T104 P094	H	11.00	13.99	18.98	922.36	88.8	5.1	0.062	0.125	897.5	
T104 P094	H	11.50	13.99	15.98	935.55	89.2	5.1	0.062	0.125	2513.3	
T104 P094	H	12.00	13.99	20.25	935.06	89.3	5.1	0.062	0.125	698.6	
T104 P094	H	12.50	13.99	17.16	944.34	89.3	5.1	0.062	0.125	1530.0	
T104 P094	H	13.00	13.99	15.66	953.61	89.5	5.1	0.062	0.125	3080.8	
T104 P094	H	13.50	13.99	15.48	959.96	89.8	5.1	0.062	0.125	3504.5	
T104 P094	H	14.00	13.99	16.03	961.91	90.1	5.1	0.062	0.125	2518.6	
T104 P094	H	14.50	13.99	16.63	970.70	90.5	5.1	0.062	0.125	1926.8	Fe cemented
T104 P094	H	15.00	13.99	16.68	971.68	90.5	5.1	0.062	0.125	1890.6	
T104 P094	H	15.50	13.99	20.90	982.91	90.3	5.1	0.062	0.125	653.3	
T104 P094	H	16.00	13.99	18.67	978.52	90.2	5.1	0.062	0.125	1026.9	
T104 P094	H	16.50	13.99	16.64	989.26	90.2	5.1	0.062	0.125	1953.7	
T104 P094	H	17.00	13.99	16.54	995.12	90.0	5.1	0.062	0.125	2046.9	
T104 P094	H	17.50	13.99	16.48	1003.42	90.2	5.1	0.062	0.125	2118.9	Fe mottling
T104 P094	H	18.00	13.99	16.57	996.09	87.5	5.1	0.062	0.125	2026.9	
T104 P094	H	18.50	13.99	17.05	1010.74	87.9	5.1	0.062	0.125	1701.9	
T104 P094	H	19.00	13.99	15.48	898.44	88.1	5.1	0.062	0.125	3278.8	
T104 P094	H	19.50	13.99	17.26	907.23	88.1	5.1	0.062	0.125	1421.2	mm-scale lamina
T104 P094	H	20.00	13.99	17.71	910.65	88.3	5.1	0.062	0.125	1235.7	mm-scale lamina

Minipermeameter Data from core T104 P094

Core	type	depth (ft)	Atm. P (psi)	Upstream P (psi)	Flow Rate (CC/mln)	Temp. (deg. F)	Geometric Factor	Tip Radius (inch.)		Ka (md)	Comments
								Inter. R	Exter. R		
T104 P094	H	20.50	13.99	17.76	915.04	88.6	5.1	0.062	0.125	1223.8	mm-scale lamina
T104 P094	H	21.00	13.99	15.81	924.81	88.8	5.1	0.062	0.125	2733.2	
T104 P094	H	22.50	13.99	31.57	385.62	89.2	5.1	0.062	0.125	77.1	highly Fe cemented
T104 P094	H	23.00	13.99	32.14	376.34	89.5	5.1	0.062	0.125	72.0	highly Fe cemented
T104 P094	H	23.50	13.99	28.00	932.13	89.2	5.1	0.062	0.125	253.7	mm-scale lamina
T104 P094	H	24.00	13.99	31.54	460.94	89.4	5.1	0.062	0.125	92.4	mm-scale lamina
T104 P094	H	24.50	13.99	21.89	950.68	89.3	5.1	0.062	0.125	537.5	
T104 P094	H	25.00	13.99	20.01	956.06	89.4	5.1	0.062	0.125	748.6	
T104 P094	H	25.50	13.99	17.98	961.43	89.2	5.1	0.062	0.125	1206.8	slightly Fe cemented
T104 P094	H	26.00	13.99	20.02	962.40	89.4	5.1	0.062	0.125	751.8	Fe cemented

Appendix 2 (cont.)

Minipermeameter Data from core T132 P014											
Core	type	depth (ft)	Atm. P (psi)	Upstream P (psi)	Flow Rate (CC/min)	Temp. (deg. F)	Geometric Factor	Tip Radius (inch.)		Ka (md)	Comments
								Inter. R	Exter. R		
T132 P014	H	2.75	14.01	16.36	1606.93	86.7	5.1	0.062	0.125	3614.4	
T132 P014	H	3.00	14.01	16.85	1615.72	87.0	5.1	0.062	0.125	2960.2	
T132 P014	H	3.25	14.01	19.82	1624.51	87.2	5.1	0.062	0.125	1323.0	
T132 P014	H	3.25	14.01	16.41	1633.79	87.5	5.1	0.062	0.125	3594.7	
T132 P014	H	3.50	14.01	18.84	1633.79	87.6	5.1	0.062	0.125	1651.8	
T132 P014	H	3.75	14.01	17.62	1656.25	87.9	5.1	0.062	0.125	2328.8	
T132 P014	H	3.75	14.01	16.83	1646.48	88.0	5.1	0.062	0.125	3031.4	
T132 P014	H	4.00	14.01	27.09	1671.39	88.3	5.1	0.062	0.125	498.2	sampled above boundary
T132 P014	H	4.00	14.01	16.65	1663.57	88.9	5.1	0.062	0.125	3295.7	sampled below boundary
T132 P014	H	4.25	14.01	33.94	1687.50	89.0	5.1	0.062	0.125	283.0	
T132 P014	H	4.25	14.01	22.86	1684.57	89.2	5.1	0.062	0.125	826.8	
T132 P014	H	4.50	14.01	19.41	1684.08	89.4	5.1	0.062	0.125	1496.0	
T132 P014	H	4.75	14.01	19.65	1691.41	89.3	5.1	0.062	0.125	1427.0	
T132 P014	H	5.00	14.01	32.17	1692.87	89.5	5.1	0.062	0.125	323.5	
T132 P014	H	5.00	14.01	25.42	1721.19	89.6	5.1	0.062	0.125	613.4	
T132 P014	H	5.25	14.01	18.10	1708.98	90.2	5.1	0.062	0.125	2084.8	
T132 P014	H	5.25	14.01	19.93	1709.96	90.4	5.1	0.062	0.125	1363.2	
T132 P014	H	5.50	14.01	22.07	1726.56	90.4	5.1	0.062	0.125	951.6	
T132 P014	H	5.75	14.01	22.85	1738.77	90.4	5.1	0.062	0.125	855.1	
T132 P014	H	6.00	14.01	20.40	1738.77	90.6	5.1	0.062	0.125	1268.2	sampled above boundary
T132 P014	H	6.00	14.01	19.43	1721.68	90.3	5.1	0.062	0.125	1521.7	sampled below boundary
T132 P014	H	6.15	13.99	21.11	1370.61	81.8	5.1	0.062	0.125	877.6	
T132 P014	H	6.15	13.99	19.26	1385.25	83.4	5.1	0.062	0.125	1263.9	
T132 P014	H	6.25	14.01	22.88	1733.40	90.3	5.1	0.062	0.125	849.5	
T132 P014	H	6.50	13.99	19.15	1396.00	85.6	5.1	0.062	0.125	1305.8	
T132 P014	H	6.70	13.99	26.69	1405.27	86.0	5.1	0.062	0.125	435.7	
T132 P014	H	6.80	13.99	19.73	1417.48	87.2	5.1	0.062	0.125	1173.4	
T132 P014	H	6.90	13.99	19.56	1422.85	87.9	5.1	0.062	0.125	1220.3	
T132 P014	H	7.10	13.99	20.79	1420.41	88.8	5.1	0.062	0.125	962.2	
T132 P014	H	7.25	13.99	19.30	1431.64	89.2	5.1	0.062	0.125	1297.4	
T132 P014	H	7.50	13.99	23.94	1440.92	89.8	5.1	0.062	0.125	611.8	
T132 P014	H	7.75	13.99	20.39	1452.15	90.3	5.1	0.062	0.125	1058.2	
T132 P014	H	7.80	13.99	22.31	1453.61	90.6	5.1	0.062	0.125	770.7	

Minipermeameter Data from core T132 P014

Core	type	depth (ft)	Atm. P (psi)	Upstream P (psi)	Flow Rate (CC/min)	Temp. (deg. F)	Geometric Factor	Tip Radius (inch.)		Ka (md)	Comments
								Inter. R	Exter. R		
T132 P014	H	8.10	13.99	35.69	1475.59	90.8	5.1	0.062	0.125	219.3	
T132 P014	H	8.50	13.99	18.62	1469.24	91.4	5.1	0.062	0.125	1560.9	
T132 P014	H	8.75	13.99	19.39	1480.47	91.5	5.1	0.062	0.125	1317.6	
T132 P014	H	8.85	13.99	18.70	1496.09	91.9	5.1	0.062	0.125	1556.7	
T132 P014	H	9.00	13.99	29.29	1510.74	92.1	5.1	0.062	0.125	365.8	
T132 P014	H	9.25	13.99	17.07	1523.44	92.3	5.1	0.062	0.125	2556.1	
T132 P014	H	9.50	13.99	23.80	1525.39	92.1	5.1	0.062	0.125	659.1	
T132 P014	H	9.75	13.99	22.35	1539.55	92.3	5.1	0.062	0.125	812.1	
T132 P014	H	10.00	13.99	20.96	1571.29	92.0	5.1	0.062	0.125	1033.8	
T132 P014	H	10.25	13.99	21.33	1558.11	92.2	5.1	0.062	0.125	963.9	
T132 P014	H	10.50	13.99	25.65	1564.94	92.6	5.1	0.062	0.125	542.9	
T132 P014	H	10.75	13.99	19.80	1591.31	92.6	5.1	0.062	0.125	1299.2	
T132 P014	H	11.00	13.99	18.75	1582.52	92.9	5.1	0.062	0.125	1627.6	
T132 P014	H	11.25	13.99	28.94	1612.31	92.8	5.1	0.062	0.125	402.6	
T132 P014	H	11.50	13.99	22.52	1609.38	92.8	5.1	0.062	0.125	628.1	
T132 P014	H	11.75	13.99	21.69	1611.33	92.8	5.1	0.062	0.125	939.8	
T132 P014	H	11.90	13.99	20.09	1611.33	93.1	5.1	0.062	0.125	1241.7	
T132 P014	H	12.00	13.98	20.15	1073.24	86.7	5.1	0.062	0.125	815.1	
T132 P014	H	12.25	13.98	17.74	1086.91	87.2	5.1	0.062	0.125	1459.6	
T132 P014	H	12.50	13.98	19.26	1098.63	88.9	5.1	0.062	0.125	1001.6	
T132 P014	H	12.75	13.98	20.53	1107.42	89.5	5.1	0.062	0.125	784.3	
T132 P014	H	12.85	13.98	17.44	1127.44	91.4	5.1	0.062	0.125	1658.7	
T132 P014	H	12.90	13.98	18.68	1135.74	91.8	5.1	0.062	0.125	1186.1	
T132 P014	H	13.00	13.98	31.87	1089.84	91.8	5.1	0.062	0.125	212.9	
T132 P014	H	13.25	13.98	20.03	1146.48	92.2	5.1	0.062	0.125	892.4	
T132 P014	H	13.50	13.98	19.43	494.26	92.0	5.1	0.062	0.125	512.5	
T132 P014	H	13.50	13.98	16.54	1280.27	92.0	5.1	0.062	0.125	2622.9	
T132 P014	H	13.75	13.98	18.09	644.53	92.6	5.1	0.062	0.125	783.2	
T132 P014	H	14.00	13.98	18.19	650.39	93.0	5.1	0.062	0.125	769.7	
T132 P014	H	14.25	13.98	15.66	654.79	93.0	5.1	0.062	0.125	2102.3	
T132 P014	H	14.50	13.98	15.89	656.74	92.8	5.1	0.062	0.125	1838.9	
T132 P014	H	14.75	13.98	19.87	664.55	92.6	5.1	0.062	0.125	533.7	
T132 P014	H	15.00	13.98	16.53	666.50	93.0	5.1	0.062	0.125	1372.8	
T132 P014	H	15.25	13.98	17.22	672.36	93.1	5.1	0.062	0.125	1063.9	
T132 P014	H	15.50	13.98	34.30	674.81	93.0	5.1	0.062	0.125	110.2	
T132 P014	H	15.75	13.98	16.39	684.57	93.9	5.1	0.062	0.125	1495.2	mica-bounded sandy lamina

Minipermeameter Data from core T132 P014

Core	type	depth (ft)	Atm. P (psi)	Upstream P (psi)	Flow Rate (CC/min)	Temp. (deg. F)	Geometric Factor	Tip Radius (inch.)		Ka (md)	Comments
								Inter. R	Exter. R		
T132 P014	H	16.00	13.98	20.17	687.50	93.6	5.1	0.062	0.125	521.6	mica-bounded sandy lamina
T132 P014	H	16.25	13.98	22.02	698.73	93.6	5.1	0.062	0.125	386.8	mica-bounded sandy lamina
T132 P014	H	16.50	13.98	15.71	693.85	93.6	5.1	0.062	0.125	2161.6	
T132 P014	H	16.75	13.98	21.48	694.82	93.8	5.1	0.062	0.125	418.4	Fe-rich
T132 P014	H	17.00	13.98	34.34	698.73	93.9	5.1	0.062	0.125	113.9	Fe-rich
T132 P014	H	17.50	13.98	24.89	706.06	93.3	5.1	0.062	0.125	266.9	Fe-rich
T132 P014	H	18.00	13.98	40.96	389.89	93.6	5.1	0.062	0.125	42.2	Fe-rich
T132 P014	H	18.25	13.98	45.57	3.42	93.5	5.1	0.062	0.125	0.3	calcite cement
T132 P014	H	18.50	13.98	45.03	6.51	93.6	5.1	0.062	0.125	0.6	calcite cement
T132 P014	H	18.75	13.98	45.70	2.61	94.0	5.1	0.062	0.125	0.2	calcite cement
T132 P014	H	19.00	13.98	45.67	3.74	94.0	5.1	0.062	0.125	0.3	calcite cement
T132 P014	H	19.25	13.98	45.94	2.42	94.2	5.1	0.062	0.125	0.2	calcite cement
T132 P014	H	19.50	13.98	45.61	3.97	94.0	5.1	0.062	0.125	0.3	calcite cement
T132 P014	H	19.75	13.98	45.09	3.58	93.3	5.1	0.062	0.125	0.3	calcite cement
T132 P014	H	20.00	13.98	45.67	4.92	92.7	5.1	0.062	0.125	0.4	calcite cement
T132 P014	H	20.25	13.98	44.15	39.49	92.8	5.1	0.062	0.125	3.6	calcite cement
T132 P014	H	20.50	13.98	40.92	457.89	92.7	5.1	0.062	0.125	49.6	calcite cement
T132 P014	H	20.75	13.98	45.92	4.46	92.8	5.1	0.062	0.125	0.4	calcite cement
T132 P014	H	21.00	13.98	45.80	5.73	93.2	5.1	0.062	0.125	0.5	calcite cement
T132 P014	H	21.25	13.98	46.20	4.18	93.3	5.1	0.062	0.125	0.3	calcite cement
T132 P014	H	21.50	13.98	45.80	4.46	93.0	5.1	0.062	0.125	0.4	calcite cement
T132 P014	H	21.75	13.98	45.41	4.14	92.9	5.1	0.062	0.125	0.4	calcite cement
T132 P014	H	22.00	13.98	46.17	4.04	93.0	5.1	0.062	0.125	0.3	calcite cement
T132 P014	H	22.25	13.98	45.22	27.67	93.6	5.1	0.062	0.125	2.4	calcite cement
T132 P014	H	22.50	13.98	46.36	7.04	93.8	5.1	0.062	0.125	0.6	calcite cement
T132 P014	H	22.75	13.98	46.47	7.75	94.0	5.1	0.062	0.125	0.6	calcite cement

Appendix 2 (cont.)

Minipermeameter Data from core T132 P046											
Core	type	depth (ft)	Atm. P (psi)	Upstream P (psi)	Flow Rate (CC/min)	Temp. (deg. F)	Geometric Factor	Tip Radius (inch.)		Ka (md)	Comments
								Inter. R	Exter. R		
T132 P046	H	7.00	14.03	16.49	890.14	84.8	5.1	0.062	0.125	1893.1	
T132 P046	H	7.50	14.03	18.03	918.46	85.7	5.1	0.062	0.125	1145.5	
T132 P046	H	8.00	14.03	18.90	927.73	86.4	5.1	0.062	0.125	926.3	
T132 P046	H	8.50	14.03	20.22	924.32	86.7	5.1	0.062	0.125	698.3	
T132 P046	H	9.00	14.03	24.13	438.11	87.2	5.1	0.062	0.125	181.9	on boundary
T132 P046	H	9.00	14.03	17.14	949.22	87.2	5.1	0.062	0.125	1566.8	above boundary
T132 P046	H	9.50	14.03	23.15	799.32	87.2	5.1	0.062	0.125	377.6	
T132 P046	H	10.00	14.03	19.51	955.08	87.4	5.1	0.062	0.125	832.1	
T132 P046	H	10.50	14.03	17.49	958.98	87.8	5.1	0.062	0.125	1405.5	Fe cemented
T132 P046	H	11.00	14.03	16.58	968.75	88.3	5.1	0.062	0.125	1987.2	
T132 P046	H	11.50	14.03	20.84	969.24	88.5	5.1	0.062	0.125	653.7	mm-scale lamina
T132 P046	H	12.00	14.03	17.31	979.98	88.6	5.1	0.062	0.125	1525.5	
T132 P046	H	12.50	14.03	16.21	994.14	88.9	5.1	0.062	0.125	2410.2	
T132 P046	H	13.00	14.03	16.30	988.77	89.0	5.1	0.062	0.125	2300.5	
T132 P046	H	13.50	14.03	18.98	996.58	89.2	5.1	0.062	0.125	975.9	mm-scale lamina
T132 P046	H	14.00	14.03	23.72	961.43	89.3	5.1	0.062	0.125	421.0	slumped
T132 P046	H	14.50	14.03	16.32	1004.88	89.4	5.1	0.062	0.125	2311.5	
T132 P046	H	15.00	14.03	16.55	1010.25	89.6	5.1	0.062	0.125	2094.6	
T132 P046	H	15.50	14.03	22.17	892.09	89.6	5.1	0.062	0.125	485.0	mm-scale lamina
T132 P046	H	16.00	14.03	18.92	893.56	89.7	5.1	0.062	0.125	887.6	laminated; Fe cemented
T132 P046	H	16.50	14.03	17.52	893.56	89.8	5.1	0.062	0.125	1300.0	slumped
T132 P046	H	17.00	14.03	19.97	901.37	89.9	5.1	0.062	0.125	714.5	slumped
T132 P046	H	17.50	14.03	16.05	905.76	90.0	5.1	0.062	0.125	2381.0	
T132 P046	H	18.00	14.03	17.40	905.76	87.0	5.1	0.062	0.125	1370.0	laminated
T132 P046	H	18.50	14.03	16.94	908.20	87.1	5.1	0.062	0.125	1609.5	laminated
T132 P046	H	19.00	14.03	16.06	913.09	87.2	5.1	0.062	0.125	2383.5	laminated
T132 P046	H	19.50	14.03	17.59	922.85	87.2	5.1	0.062	0.125	1311.3	mm-scale lamina
T132 P046	H	20.00	14.03	18.07	931.64	87.3	5.1	0.062	0.125	1150.5	
T132 P046	H	20.50	14.03	16.31	938.48	87.5	5.1	0.062	0.125	2170.3	
T132 P046	H	21.00	14.03	18.27	950.20	87.5	5.1	0.062	0.125	1108.9	
T132 P046	H	21.50	14.03	15.64	948.24	87.7	5.1	0.062	0.125	3177.0	
T132 P046	H	22.00	14.03	16.13	1303.22	88.1	5.1	0.062	0.125	3296.9	
T132 P046	H	22.50	14.03	17.11	916.99	88.2	5.1	0.062	0.125	1527.1	Fe mottling

Minipermeameter Data from core T132 P046

Core	type	depth (ft)	Atm. P (psi)	Upstream P (psi)	Flow Rate (CC/min)	Temp. (deg. F)	Geometric Factor	Tip Radius (inch.)		Ka (md)	Comments
								Inter. R	Exter. R		
T132 P046	H	23.00	14.03	24.78	921.39	88.3	5.1	0.062	0.125	353.6	Fe mottling
T132 P046	H	23.50	14.03	36.21	112.92	88.6	5.1	0.062	0.125	16.2	Fe cemented conglomerate
T132 P046	H	24.00	14.03	34.01	403.44	88.4	5.1	0.062	0.125	87.3	Fe cemented
T132 P046	H	24.50	14.03	40.64	2.25	89.3	5.1	0.062	0.125	0.2	calcite cemented conglomerate
T132 P046	H	25.00	14.03	39.58	2.88	89.9	5.1	0.062	0.125	0.3	calcite cemented sandstone
T132 P046	H	25.50	14.03	40.04	3.43	90.3	5.1	0.062	0.125	0.4	calcite cemented conglomerate
T132 P046	H	26.00	14.03	35.41	295.90	89.9	5.1	0.062	0.125	44.8	silty conglomeratic sandstone
T132 P046	H	26.50	14.03	40.45	2.54	90.2	5.1	0.062	0.125	0.3	Fe cemented conglomerate
T132 P046	H	26.90	14.03	33.53	689.94	90.2	5.1	0.062	0.125	119.2	Fe cemented sandstone

Appendix 3 - Data for Laboratory Core Plugs - Horizontal Ka measurements													
Minipermeameter Data										Laboratory Data			
Core #	depth (ft)	Atm. P (psi)	Upstream P (psi)	Flow Rate (CC/mln)	Temp. (deg. F)	Geometric Factor	Tip Radius (inch.)		Ka (md)	Ka (md)	Porosity (%)	Grain Density (g/cc)	Comments
							Inter. R	exter. R					
T132 P014	2.9	13.97	16.65	1437.50	87.3	5.1	0.062	0.125	2799.7	2622.0	36.4	2.70	
T132 P014	4.1	13.97	16.42	1477.05	90.0	5.1	0.062	0.125	3174.4	3192.0	36.4	2.69	
T132 P014	5.2	13.97	16.52	1501.47	90.8	5.1	0.062	0.125	3093.9	2345.0	35.4	2.67	
T132 P014	6.2	13.97	19.93	1519.04	91.1	5.1	0.062	0.125	1203.0	1204.0	35.2	2.70	
T132 P014	7.0	13.97	18.88	1525.39	91.4	5.1	0.062	0.125	1512.7	1296.0	35.8	2.69	
T132 P014	7.9	13.97	23.41	1543.95	92.0	5.1	0.062	0.125	700.7	656.0	33.3	2.67	
T132 P014	8.9	13.97	19.36	1557.62	91.7	5.1	0.062	0.125	1388.3	1590.0	33.0	2.68	
T132 P014	10.0	13.97	19.68	1572.75	91.5	5.1	0.062	0.125	1311.4	1665.0	33.7	2.68	
T132 P014	10.9	13.97	18.59	1577.15	92.1	5.1	0.062	0.125	1338.6	1637.0	33.4	2.68	
T132 P014	11.9	13.97	18.80	1588.38	92.5	5.1	0.062	0.125	1607.5	1672.0	30.8	2.67	
T132 P014	12.9	13.97	20.14	1601.07	92.6	5.1	0.062	0.125	1218.2	1350.0	30.8	2.67	
T132 P014	14.0	13.97	24.18	1625.49	92.6	5.1	0.062	0.125	668.5	900.0	29.7	2.68	
T132 P014	15.0	13.97	20.07	1617.19	92.9	5.1	0.062	0.125	1248.0	1375.0	33.1	2.68	
T132 P014	17.0	13.97	48.46	1198.73	93.2	5.1	0.062	0.125	97.9	168.0	45.0	2.76	cemented
T132 P014	18.0	13.97	46.40	1379.88	93.5	5.1	0.062	0.125	113.0	80.0	48.2	2.79	cemented
T132 P014	19.0	13.97	49.99	3.74	93.7	5.1	0.062	0.125	0.3	0.02	4.0	2.66	cemented
T132 P014	20.0	13.97	49.99	4.48	94.2	5.1	0.062	0.125	0.3	0.04	9.3	2.78	cemented
T132 P014	21.0	13.97	49.99	4.52	94.6	5.1	0.062	0.125	0.3	0.01	2.0	2.68	cemented
T132 P014	22.0	13.97	49.99	5.73	93.9	5.1	0.062	0.125	0.4	0.04	6.9	2.69	cemented
T132 P014	23.0	13.97	49.99	2.21	94.1	5.1	0.062	0.125	0.2	0.01	7.5	2.72	cemented
T104 P014	2.8	13.97	15.96	1261.72	90.6	5.1	0.062	0.125		1767.0	36.2	2.66	frac. before miniK
T104 P014	3.8	13.97	20.26	1273.93	91.1	5.1	0.062	0.125	946.9	1023.0	36.6	2.66	
T104 P014	4.8	13.97	17.19	1294.92	91.6	5.1	0.062	0.125	2067.1	1455.0	34.0	2.66	
T104 P014	5.8	13.97	18.07	1299.32	91.8	5.1	0.062	0.125	1585.0	1292.0	34.8	2.67	
T104 P014	6.8	13.97	16.63	1313.97	92.4	5.1	0.062	0.125	2587.1	2088.0	33.7	2.67	
T104 P014	7.8	13.97	17.58	1331.06	92.8	5.1	0.062	0.125	1872.1	1692.0	35.1	2.65	
T104 P014	8.8	13.97	17.83	1340.82	92.9	5.1	0.062	0.125	1746.7	1644.0	35.5	2.66	
T104 P014	9.8	13.97	18.80	1363.77	92.8	5.1	0.062	0.125	2509.3	2003.0	35.8	2.67	
T104 P014	11.9	13.97	18.45	1376.95	92.8	5.1	0.062	0.125	1520.2	1213.0	35.6	2.68	
T104 P014	12.8	13.97	16.80	1387.70	93.0	5.1	0.062	0.125	2553.5	2592.0	36.7	2.67	
T104 P014	13.8	13.97	38.20	979.49	93.2	5.1	0.062	0.125	124.2	136.0	35.5	2.73	cemented
T104 P014	14.7	13.97	42.93	5.14	93.9	5.1	0.062	0.125	0.5	0.04	8.4	2.71	cemented
T104 P014	15.9	13.97	43.84	1.39	94.1	5.1	0.062	0.125	0.1	0.04	4.3	2.66	cemented
T104 P014	16.7	13.97	42.99	7.20	94.3	5.1	0.062	0.125	0.7	0.58	12.5	2.71	cemented congl.
T104 P014	18.1	13.97	19.95	1404.30	94.1	5.1	0.062	0.125	1110.0	1384.0	32.7	2.67	
T104 P014	18.9	13.97	18.47	1417.48	94.1	5.1	0.062	0.125	1555.6	1562.0	32.1	2.66	
T104 P014	19.9	13.97	20.04	1425.29	94.1	5.1	0.062	0.125	1105.3	1102.0	29.7	2.69	

Appendix 4 - Thin section analyses of Hwy 7 cores behind outcrop. Locations of cores are shown in Figure 4.

Thin section locations are shown to the right of core descriptions in Appendix 1 and on Plate 1.

Core #	Thin section #	Sample Depth (ft)	Avg. Qtz. Grain Size (mm)	Sorting	Approx. sphericity Index	roundness	mlca (%)	clay (%)	cement (%)	Comments	Porosity (%)	Ka (md)	Grain Density (g/cc)
T132P014	1	2.9	0.17	well sorted	0.75	subrounded	2.00	0.50	4.00	Fe-oxide cement	36.4	2622	2.70
T132P014	2	4.1	0.15	well sorted	0.71	subrounded	2.25	0.75	2.00	Fe-oxide cement	36.4	3192	2.69
T132P014	3	5.2	0.14	well sorted	0.67	subangular	4.00	1.00	4.00	Fe-oxide cement	35.4	2345	2.67
T132P014	4	6.2	0.11	moderately sorted	0.69	subangular	4.75	1.00	3.00	Fe-oxide cement	35.2	1204	2.70
T132P014	5	7.0	0.12	well sorted	0.71	subangular	6.25	1.50	3.00	Fe-oxide cement	35.8	1296	2.69
T132P014	6	7.9	0.11	well sorted	0.67	subangular	8.50	2.00	3.00	Fe-oxide cement	33.3	656	2.67
T132P014	7	8.9	0.14	very well sorted	0.71	subrounded	2.50	1.50	4.00	Fe-oxide cement	33.0	1590	2.68
T132P014	8	10.0	0.14	very well sorted	0.71	subrounded	2.75	2.00	3.00	Fe-oxide cement	33.7	1665	2.68
T132P014	9	10.9	0.12	very well sorted	0.69	subrounded	2.00	3.00	4.00	Fe-oxide cement	33.4	1637	2.68
T132P014	10	11.9	0.15	very well sorted	0.73	subrounded	1.75	2.00	4.00	Fe-oxide cement	30.8	1672	2.67
T132P014	11	12.9	0.14	well sorted	0.71	subangular	4.25	3.00	5.00	Fe-oxide cement	30.8	1350	2.67
T132P014	12	14.0	0.09	well sorted	0.67	subangular	5.25	5.00	3.00	Fe-oxide cement	29.7	900	2.68
T132P014	13	15.0	0.14	well sorted	0.71	subangular	4.25	5.00	3.00	Fe-oxide cement	33.1	1375	2.68
T132P014	14	17.0	0.17	very well sorted	0.73	subrounded	1.25	4.00	40.00	Fe-oxide cement	45.0	168	2.76
T132P014	15	18.0	0.14	very well sorted	0.73	subrounded	0.75	6.00	50.00	Fe-oxide cement; shale clasts	48.2	80	2.79
T132P014	16	19.0	0.15	very well sorted	0.71	subrounded	1.38	3.00	40.00	calcite cement; shale clasts	4.0	0.02	2.66
T132P014	17	20.0	0.09	very poorly sorted	0.67	subangular	0.50	20.00	30.00	calcite cemented cgl.	9.3	0.04	2.78
T132P014	18	21.0	0.09	very well sorted	0.73	rounded	0.75	1.00	45.00	calcite cement	2.0	0.01	2.68
T132P014	19	22.0	0.11	very well sorted	0.65	subangular	0.50	2.00	45.00	calcite cement; Fe-oxide cement	6.9	0.04	2.69
T132P014	20	22.9	0.12	well sorted	0.69	subrounded	0.75	4.00	30.00	Fe-oxide cement; shale clasts	7.5	0.01	2.72
T104P014	21	2.8	0.12	well sorted	0.71	subrounded	2.25	2.00	2.00	Fe-oxide cement	36.2	1767	2.66
T104P014	22	3.8	0.11	moderately sorted	0.73	subangular	6.25	4.00	5.00	Fe-oxide cement	36.6	1023	2.66
T104P014	23	4.8	0.12	well sorted	0.71	subrounded	3.75	2.50	2.00	Fe-oxide cement	34.0	1455	2.66
T104P014	24	5.8	0.12	moderately sorted	0.69	subangular	6.25	4.00	3.00	Fe-oxide cement	34.8	1292	2.67
T104P014	25	6.8	0.15	well sorted	0.71	subrounded	1.50	2.00	5.00	Fe-oxide cement	33.7	2088	2.67
T104P014	26	7.8	0.14	well sorted	0.71	subrounded	1.25	4.00	3.00	Fe-oxide cement; shale clasts	35.1	1692	2.65
T104P014	27	8.8	0.14	well sorted	0.73	subrounded	3.00	3.00	2.00	Fe-oxide cement	35.5	1644	2.66
T104P014	28	9.8	0.15	well sorted	0.75	subrounded	2.25	4.00	3.00	Fe-oxide cement	35.8	2003	2.67
T104P014	29	11.9	0.14	well sorted	0.73	subrounded	1.50	5.00	12.00	Fe-oxide cement	35.6	1213	2.68
T104P014	30	12.8	0.15	well sorted	0.71	subangular	1.13	2.00	2.00	Fe-oxide cement	36.7	2592	2.67
T104P014	31	13.8	0.12	well sorted	0.69	subangular	3.00	4.00	20.00	Fe-oxide cement	35.5	136	2.73
T104P014	32	14.7	0.14	well sorted	0.73	subangular	1.13	2.00	40.00	Fe-oxide cement; calcite cement	8.4	0.04	2.71
T104P014	33	15.9	0.12	moderately sorted	0.67	subrounded	0.75	6.00	45.00	calcite cement; shale clasts	4.3	0.04	2.66
T104P014	34	16.7	0.14	well sorted	0.71	subrounded	0.63	8.00	35.00	calcite and Fe-oxide cement; shale clasts	12.5	0.58	2.71
T104P014	35	18.1	0.11	well sorted	0.73	subrounded	1.13	2.00	4.00	Fe-oxide cement	32.7	1384	2.67
T104P014	36	18.9	0.12	well sorted	0.75	subrounded	0.88	2.00	4.00	Fe-oxide cement	32.1	1562	2.68
T104P014	37	19.9	0.11	well sorted	0.75	subrounded	0.75	2.00	5.00	Fe-oxide cement	29.7	1102	2.69

Appendix 5 - Lab and minipermeameter Ka values and statistics for plugs

All Samples				
Core #	Depth (ft)	LabK Ka (md)	miniK Ka (md)	% differ.
T132 P014	2.9	2622.0	2799.7	#REF!
T132 P014	4.1	3192.0	3174.4	#REF!
T132 P014	5.2	2345.0	3093.9	#REF!
T132 P014	6.2	1204.0	1203.0	#REF!
T132 P014	7.0	1296.0	1512.7	#REF!
T132 P014	7.9	656.0	700.7	#REF!
T132 P014	8.9	1590.0	1388.3	#REF!
T132 P014	10.0	1665.0	1311.4	#REF!
T132 P014	10.9	1637.0	1338.6	#REF!
T132 P014	11.9	1672.0	1607.5	#REF!
T132 P014	12.9	1350.0	1218.2	#REF!
T132 P014	14.0	900.0	668.5	#REF!
T132 P014	15.0	1375.0	1248.0	#REF!
T132 P014	17.0	168.0	97.9	#REF!
T132 P014	18.0	80.0	113.0	#REF!
T132 P014	19.0	0.02	0.3	
T132 P014	20.0	0.04	0.3	
T132 P014	21.0	0.01	0.3	
T132 P014	22.0	0.04	0.4	
T132 P014	22.9	0.01	0.2	
T104 P014	3.8	1023.0	946.9	#REF!
T104 P014	4.8	1455.0	2067.1	#REF!
T104 P014	5.8	1292.0	1585.0	#REF!
T104 P014	6.8	2088.0	2587.1	#REF!
T104 P014	7.8	1692.0	1872.1	#REF!
T104 P014	8.8	1644.0	1746.7	#REF!
T104 P014	9.8	2003.0	2509.3	#REF!
T104 P014	11.9	1213.0	1520.2	#REF!
T104 P014	12.8	2592.0	2553.5	#REF!
T104 P014	13.8	136.0	124.2	#REF!
T104 P014	14.7	0.04	0.5	
T104 P014	15.9	0.04	0.1	
T104 P014	16.7	0.58	0.7	
T104 P014	18.1	1384.0	1110.0	#REF!
T104 P014	18.9	1562.0	1555.6	#REF!
T104 P014	19.9	1102.0	1105.3	#REF!

Uncemented Samples Laboratory Analyses			
Core #	Depth (ft)	Porosity (%)	Ka (md)
T132P014	2.9	36.4	2622.0
T132P014	4.1	36.4	3192.0
T132P014	5.2	35.4	2345.0
T132P014	6.2	35.2	1204.0
T132P014	7.0	35.8	1296.0
T132P014	7.9	33.3	656.0
T132P014	8.9	33.0	1590.0
T132P014	10.0	33.7	1665.0
T132P014	10.9	33.4	1637.0
T132P014	11.9	30.8	1672.0
T132P014	12.9	30.8	1350.0
T132P014	14.0	29.7	900.0
T132P014	15.0	33.1	1375.0
T104P014	2.8	36.2	1767.0
T104P014	3.8	36.6	1023.0
T104P014	4.8	34.0	1455.0
T104P014	5.8	34.8	1292.0
T104P014	6.8	33.7	2088.0
T104P014	7.8	35.1	1692.0
T104P014	8.8	35.5	1644.0
T104P014	9.8	35.8	2003.0
T104P014	11.9	35.6	1213.0
T104P014	12.8	36.7	2592.0
T104P014	18.1	32.7	1384.0
T104P014	18.9	32.1	1562.0
T104P014	19.9	29.7	1102.0

Uncemented Samples Laboratory Analyses		
Ka Statistics		Phi Statistics
<i>n</i>	26	26
Geom. Mean	1537.53	
Arithmetic Mean	1627.73	34.06
Standard Error	112.22	0.42
Median	1576.00	34.40
Standard Deviation	572.22	2.12
Sample Variance	327437.88	4.50
Kurtosis	1.18	-0.45
Skewness	0.99	-0.70
Range	2536.00	7.00
Minimum	656.00	29.70
Maximum	3192.00	36.70
Sum	42321.00	885.50

Uncemented Samples Minipermeameter Analyses	
Ka Statistics	
<i>n</i>	25
Geom. Mean	1560.74
Mean	1696.95
Standard Error	142.40
Median	1520.18
Standard Deviation	712.00
Sample Variance	506937.39
Kurtosis	-0.39
Skewness	0.73
Range	2505.89
Minimum	668.50
Maximum	3174.39
Sum	42423.82

Appendix 6 - Regression statistics comparing lab and minipermeameter Ka values

Minipermeameter Ka versus Laboratory Ka						Obs. #	Predicted Y	Residuals
<i>Regression Statistics</i>						1	2777.2	22.5
Multiple R	0.9704					2	3387.3	-213.0
R Square	0.9416					3	2480.7	613.2
Adjusted R Square	0.9399					4	1259.3	-56.4
Standard Error	239.56					5	1357.8	154.9
Observations	36					6	672.8	27.9
ANOVA						7	1672.5	-284.2
	<i>df</i>	<i>SS</i>	<i>MS</i>	<i>F</i>	<i>Significance F</i>	8	1752.8	-441.4
Regression	1	31450941.0	31450941.0	548.0	1.5005E-22	9	1722.8	-384.2
Residual	34	1951184.6	57387.8			10	1760.3	-152.8
Total	35	33402125.6				11	1415.6	-197.4
						12	933.9	-265.4
						13	1442.4	-194.4
	<i>Coefficients</i>	<i>Standard Error</i>	<i>t Stat</i>	<i>P-value</i>		14	150.4	-52.5
Intercept	-29.45	65.5577	-0.4492	0.6562		15	56.2	56.8
Slope	1.0704	0.0457	23.4103	1.5005E-22		16	-29.4	29.7
						17	-29.4	29.7
						18	-29.4	29.7
	<i>Lower 95%</i>	<i>Upper 95%</i>	<i>Lower 95.0%</i>	<i>Upper 95.0%</i>		19	-29.4	29.8
Intercept	-162.67	103.78	-162.67	103.78		20	-29.4	29.6
Slope	0.9775	1.1633	0.9775	1.1633		21	1085.6	-118.7
						22	1528.0	539.1
						23	1353.5	231.5
						24	2205.6	381.6
						25	1781.7	90.3
						26	1730.3	16.4
						27	2114.6	394.7
						28	1269.0	251.2
						29	2745.1	-191.6
						30	116.1	8.1
						31	-29.4	29.9
						32	-29.4	29.5
						33	-28.8	29.5
						34	1452.0	-342.0
						35	1642.6	-86.9
						36	1150.2	-44.8